Energy & Environmental Science

Cite this: DOI: 10.1039/c1ee01263k

www.rsc.org/ees

REVIEW

Understanding and recent development of carbon coating on $LiFePO_4$ cathode materials for lithium-ion batteries

Jiajun Wang and Xueliang Sun*

Received 7th March 2011, Accepted 6th October 2011
DOI: 10.1039/c1ee01263k

Olivine-structured $LiFePO_4$ has been the focus of research in developing low cost, high performance cathode materials for lithium ion batteries. Various processes have been developed to synthesize $LiFePO_4$ or $C/LiFePO_4$ (carbon coating on $LiFePO_4$), and some of them are being used to mass produce $C/LiFePO_4$ at the commercial or pilot scale. Due to the low intrinsic electronic and ionic conductivities of $LiFePO_4$, the decrease of particle size and the nano-layer of carbon coating on $LiFePO_4$ particle surfaces are necessary to achieve a high electrochemical performance. Significant progress has been made in understanding and controlling phase purity, particle size and carbon coating of the $C/LiFePO_4$ composite material in the past. However, there are still many challenges in achieving a high quality product with high consistency. In this review, we summarize some of the recent progress and advances based on selected reports from peer-reviewed journal publications. Several typical synthesis methods and the effect of carbon coating quality on the properties of $C/LiFePO_4$ composite are reviewed. An insight into the future research and further development of $C/LiFePO_4$ composite is also discussed.

1. Introduction

Lithium-ion rechargeable batteries are the most promising power system that can offer a higher operative voltage and energy density compared to other rechargeable battery systems such as the widely used nickel metal hydride (NiMH) batteries being used in commercial hybrid electric vehicles (HEV). In recent years, there has been a dramatic increase in research and commercialization activities of lithium ion batteries for large scale energy storage and for on-board energy storage in electric vehicles (EV) and plug-in hybrid electric vehicles (PHEV).[1,2] Challenges remain in making low cost, high-performance and high-safety lithium ion batteries for vehicle applications.[3,4]

Among the components in lithium-ion batteries, the cathode material has attracted much attention because it has a significant impact on battery capacity, cycle life, safety and cost structure.[5] Due to its high capacity $LiCoO_2$ has been widely used in small batteries for portable electronics since its introduction to the market by Sony Inc. in 1991. However, its use in large size batteries has been vetoed by safety concerns. In addition to the

Dept. of Mechanical and Materials Engineering, University of Western Ontario, London, Ontario, N6A 5B9, Canada. E-mail: xsun@eng.uwo.ca; Fax: +1-519-661-3020; Tel: +1-519-661-2111 ext. 87759

Broader context

The threats arising from limited oil storage and global warming have forced us to look for alternative energy storage and conversion systems. In addition, the rapid pace and progress of the portable electronics and electric vehicles technique demand a powerful energy storage system with high energy density and high safety as well as low cost. Following two decades of development, rechargeable lithium-ion batteries (LIB) are considered as the most promising energy storage technology. Nowadays, consumer demand is motivating tremendous efforts for high capacity, high power density, fast recharging rate, and great cycling performance. However, these demands bring many challenges to material stability, especially when they are used in electric vehicles (EV). Compared with other cathode materials, olivine-type $LiFePO_4$ draws extensive attention because of its high theoretical capacity, environmental acceptability, and low cost, especially superior thermal stability and safety. The major drawback for $LiFePO_4$ is the intrinsically poor conductivity, which is currently being overcome by coating them with conductive carbon. Carbon coating is a critical component in $C/LiFePO_4$ composites. A deep and comprehensive understanding of carbon coating and its effects as well as the synthesis process to control carbon coating on $LiFePO_4$ will contribute to the LIB industry and accelerate the commercialization of EV.

safety risks, the high cost, toxicity, and environmental concerns prohibit the large scale applications of $LiCoO_2$ material in HEV, PHEV or EV. Other materials including lithium nickel manganese cobalt (NMC), lithium nickel cobalt aluminium (NCA), lithium manganese spinel and olivine lithium iron phosphate are being investigated and commercialized for various applications. Each one has advantages and disadvantages.[6–9] $LiFePO_4$ is of particular interest for use in large size batteries, due to its intrinsic structural and chemical stability that leads to safe and long cycle life batteries. Besides, olivine $LiFePO_4$ is composed of low cost and environmentally benign Fe and PO_4 moieties, which is an important merit for large scale applications. One of the main obstacles for practical applications of $LiFePO_4$ is its poor rate capability, which can be attributed to slow kinetics of lithium-ion diffusion coefficient (10^{-14} to 10^{-16} cm^2 s^{-1}) and the poor electronic conductivity (<10^{-9} s cm^{-1}).[10,11]

Since the pioneering work of John Goodenough and coworkers,[12–15] numerous works have been done to investigate the synthesis, structure, defects and physical, chemical and electrochemical properties of $LiFePO_4$. Some review articles or book/chapters were published concerning the synthesis and properties of lithium iron phosphate.[16–18] In the present work, focus is given to the C/$LiFePO_4$ and the impact of carbon precursors on the synthesis and electrochemical performance of C/$LiFePO_4$. An insight into the future research and development of C/$LiFePO_4$ composites is also discussed.

2. The structure and physical/chemical properties of pristine $LiFePO_4$

The olivine structure of $LiFePO_4$ crystal consists of a polyoxyanionic framework containing LiO_6 octahedra, FeO_6 octahedra and PO_4 tetrahedra. Strong P–O covalent bonds in $(PO_4)^{3-}$ polyanion stabilize the oxygen when fully charged and avoid O_2 release at high states of charge making $LiFePO_4$ an excellent, stable and safe cathode material (Fig. 1).[15]

The cation arrangement in $LiFePO_4$ differs from that in layered $LiCoO_2$ or spinel $LiMn_2O_4$. The divalent Fe^{2+} ions occupy the corner-shared octahedra. The P^{5+} is located in tetrahedral sites, and Li^+ resides in chains of edge-shared octahedra. The skeleton of PO_4 polyanions is very stable thermally, but the corner-shared FeO_6 octahedra of $LiFePO_4$ are separated by the oxygen atoms of the PO_4^{3-} tetrahedra and cannot form a continuous FeO_6 network, which results in the poor electronic conductivity of $LiFePO_4$.[20] At room temperature, the electronic conductivity of pristine $LiFePO_4$ is only 10^{-9} to 10^{-10} S cm^{-1},[21] which is much lower than those of $LiCoO_2$ ($\sim10^{-3}$ S cm^{-1}) and $LiMn_2O_4$ (2×10^{-5} to 5×10^{-5} S cm^{-1}).[22,23]

Atomistic modeling and first-principle calculations indicate that the lowest Li migration energy is found for the pathway along the [010] channel, with a nonlinear, curved trajectory between adjacent Li sites (Fig. 2).[24,25] Although the theoretical calculation showed that the intrinsic ionic diffusion coefficient is as high as 10^{-8} ($LiFePO_4$) to 10^{-7} ($FePO_4$) cm^2 s^{-1}, the one-dimensional channels are easily blocked by defects and impurities because blockages in one-dimensional paths are different from those in two-dimensional and three-dimensional paths where Li ions can move around the blocked sites.[26] The ionic diffusion coefficients in $LiFePO_4$ are therefore lower than the theoretical value. For example, the diffusion coefficients were reported by Takeda *et al.* in a wide range of 10^{-14} to 10^{-12} cm^2 s^{-1} with the potentiostatic intermittent titration technique, 10^{-15} to 10^{-12} cm^2 s^{-1} with electrochemical impedance spectroscopy, and 10^{-14} cm^2 s^{-1} with cyclic voltammetry, respectively.[27] A

Jiajun Wang

Jiajun Wang is presently a post-doctoral fellow at Prof. Xueliang (Andy) Sun's Nanomaterials and Energy Group at the University of Western Ontario, Canada. He received his PhD in electrochemistry from Harbin Institute of Technology (Harbin, China) in 2008 working on synthesis and application of highly stable electrode materials for fuel cell systems. His current research focuses on development of advanced Cl $LiFePO_4$ cathode for lithium-ion batteries, collaborating with Phostech Lithium Inc. as well as the study of novel electrode materials for lithium-air batteries. He has broad research interest and experience in nanomaterial fabrication and characterization, electrochemistry, and clean energy techniques. He has authored and co-authored over 20 refereed journal publications and has around 300 citations to his work.

Xueliang Sun

Professor Xueliang (Andy) Sun is a Canada Research Chair and Associate Professor at the University of Western Ontario, Canada. Dr Sun received his PhD in Materials Chemistry under the direction of Prof. George Thompson in 1999 at the University of Manchester, UK, followed by work as a post-doctoral fellow under the direction of Prof. Keith Mitchell at the University of British Columbia, Canada and as a Research Associate under the direction of Prof. Jean-Pol Dodelet at l'Institut national de la recherche scientifique (INRS), Canada. His current research interests are associated with synthesis of nanomaterials for electrochemical energy storage and conversion. His focus is on design and synthesis of various one-dimensional nanostructures such as nanotubes and nanowires as well as their composites with nanoparticles and thin films as electrocatalysis and catalyst support in fuel cells and as anode and cathodes in lithium ion batteries and Li-air batteries.

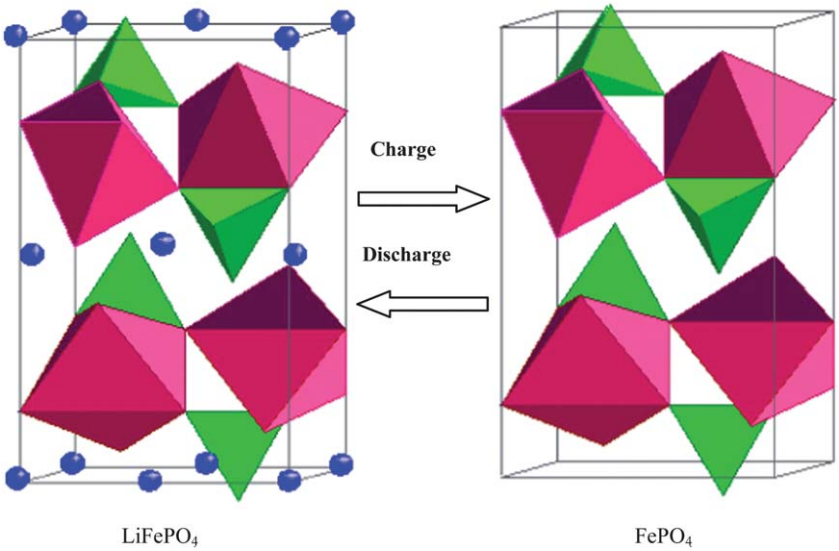

Fig. 1 The olivine structure is stable during Li-ions insertion and extraction.

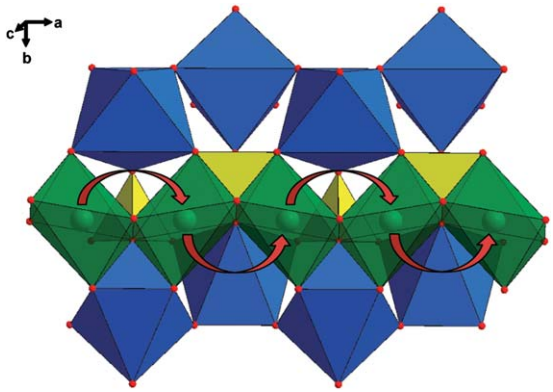

Fig. 2 Structure of $LiFePO_4$ depicting the curved trajectory of Li ion transport along the *b*-axis, shown with red arrows. The iron octahedra are shown in blue, the phosphate tetrahedral in yellow, and the lithium ions in green. Reproduced with permission from ref. 24. Copyright 2010 American Chemical Society.

lower diffusion coefficient (10^{-15} to 10^{-12} cm^2 s^{-1}) was also found in another report using the similar techniques.[28] Nevertheless, it should be mentioned that it is very difficult to accurately measure the diffusion coefficient of Li-ion in $LiFePO_4$ by these methods due to a very flat charge–discharge potential induced by the phase transformation between $LiFePO_4$ and $FePO_4$.[29]

Apparently, the low electronic and low ionic conductivities dictate the slow kinetics of charge and discharge. Various models are proposed to explain the mechanism and kinetics of charge and discharge, like the shrinking core model, domino-cascade model and the recent spinodal decomposition model.[30–32] Debates are still going on concerning the rate limiting step in the charge and discharge processes. Irrespective of those debates, various approaches towards mitigating the slow ionic and electronic conductivities are proposed and explored.

3. Various approaches to improve the performance of $LiFePO_4$

3.1 Size reduction

Size reduction to nanoscale dimension has been pointed out by John Goodenough *et al.* as one of the effective methods to solve the kinetic problems of $LiFePO_4$.[13] Nanosize pristine $LiFePO_4$ has been synthesized by hydrothermal reaction under mild conditions, which indeed shows desirable electrochemical properties when the nanoparticles are well connected with the current collectors by using a large amount of carbon particle additives.[33–35] The carbon particles play the role of forming a conductive network in the cathode coating to improve the electron transport.

Many other studies have been conducted to mitigate lithium diffusion limitations in $LiFePO_4$ by reducing particle size to shorten the diffusion length. Recent studies also show that ionic diffusion constant depends on particle size with diffusion in nanosized particles being much faster than in micrometre-sized

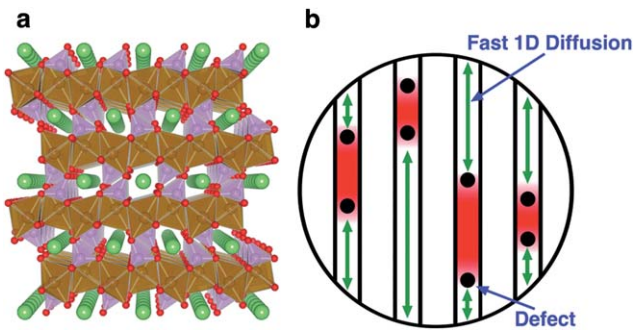

Fig. 3 (a) Crystal structure of $LiFePO_4$ illustrating 1D Li^+ diffusion channels oriented along the [010] direction. (b) Schematic illustration of Li^+ diffusion impeded by immobile point defects in 1D channels. Reproduced with permission from ref. 35. Copyright 2010 American Chemical Society.

particles or bulk (Fig. 3).[36] However, the higher surface area arising from the smaller nanoparticle size also results in other undesirable effects such as low material packing density in the cathode and potential electrode/electrolyte reactions.[37,38] An alternative effective method to improve the lithium-ion diffusion is using a higher operating temperature. However, not only the lithium-ion diffusion rate increases at high temperature, but also many undesirable reactions occur at the same time.[39] Besides the benefit of short diffusion length in the nano-sized particles, it was reported that coexisting crystalline phases have greater mutual solubility for lithium (reduced miscibility gap) in nanoscale $LiFePO_4$.[40] At higher temperatures of 100–200 °C, a solid solution is formed. In this case, a fast diffusion is expected during charge and discharge since no phase boundaries are involved.[41]

Although the size reduction strategy has been employed to improve the performance of $LiFePO_4$ in many studies, recent reports indicate that the specific capacity of $LiFePO_4$ has no clear dependence on the particle size in the range of 50–400 nm.[42,43] For example, with the introduction of highly conductive carbon, some $LiFePO_4$ materials with a larger particle size (150–300 nm) exhibited better performance than the materials of smaller size (30–100 nm). This is because Li-ion transport in these $LiFePO_4$ particles is not diffusion-controlled, and the contribution of size reduction to the capacity of $LiFePO_4$ is therefore limited.[42]

It has to be pointed out that the nano-sized particles do not necessarily always give excellent electrochemical performance. For instance, it was found that in the hydrothermal synthesis anti-site defects may form, which block lithium ion transportation, causing slow kinetics.[44] Therefore, an optimum particle size is crucial to high-performance of $LiFePO_4$, considering these adverse effects of nanosize $LiFePO_4$ in the practical applications. A particle size range of 200–400 nm was suggested in some reports for the high quality powder-based applications.[42]

3.2 Conductive surface coating

Coating of the $LiFePO_4$ surface with Cu, Ag, carbon, or conducting polymers is very effective in improving the electronic conductivity of the powders.[45] Although metal additives may effectively improve the conductivity of $LiFePO_4$, it is difficult to achieve a uniform metal dispersion on the surface of $LiFePO_4$.[45] Metal oxidation to form insulating films or soluble ions that might interfere with the negative electrode cyclability is also to be taken into account while carbon is well known for its stability and compatibility and use in practical composite cathode. Furthermore, use of a high-cost metal additive is not suitable for large-scale applications of the $LiFePO_4$ products. The conductive polymers such as polypyrrole generally have poor mechanical properties and instability.[46] Although recently poly-(3,4-ethylenedioxythiophene) (PEDOT) chemically grown on partially delitiated $LiFePO_4$ seems to lead to good cyclability,[47] by comparison, carbon coating has been particularly attractive with respect to its high conductivity using carbon concentrations as low as 0.5–2 wt%,[50–53] its low cost, and simplicity of introduction during or after the $LiFePO_4$ synthesis and most importantly its proven use as a conductivity additive in composite electrodes and its chemical stability in the battery. A combination of carbon coating and fine particle size can improve the rate performance and material utilization for $LiFePO_4$[54–56] and has been commercialized.[13,56] To make high capacity, low cost $LiFePO_4$ batteries with a suitable size, it is desirable to reduce the amount of carbon and improve the carbon coating quality. Although numerous reports in the literature have focused on C/$LiFePO_4$ composite materials and great progress has been achieved in this field in the recent years (Fig. 4),[57,58] the state-of-art understanding of the role of carbon in the C/$LiFePO_4$ composite material is still scarce.

3.3 Lattice engineering

Doping with supervalent cations in $LiFePO_4$ was first mentioned by Goodenough–Armand and reported by Chiang's group as an efficient method to improve the bulk conductivity and an increase of eight orders of magnitude in electronic conductivity was shown.[15,63] Later on, Ravet *et al.* showed that the electronic conductivity increase may come from the residual carbon from the organic precursors being used.[64] Nazar's group reported that a nano-network of metal-rich phosphides might also contribute to the enhanced conductivity.[65] Islam *et al.* investigated the doping behavior with atomistic simulation techniques and indicated that supervalent doping (*e.g.*, Ga^{3+}, Ti^{4+}, Nb^{5+}) on either Li or M sites is energetically unfavorable and does not result in a large increase in electronic (small polaron) species.[66] Clearly, the effectiveness of doping supervalent elements has been under debate since the beginning, and it is still not proven to this day.

In addition to the supervalent cation doping, it has been reported that anion doping (*e.g.* F^-, Cl^-) was also effective in enhancing the electrochemical performance of C/$LiFePO_4$. For example, F-substitution ($LiFe(PO_4)_{0.9}F_{0.3}$/C) may improve the electric conductivity of $LiFePO_4$ and alleviate the polarization under high current densities.[67] Also the high ionicity of F^- may contribute to the diffusion of lithium ion in the F-doped $LiFePO_4$.[68] However, the detailed mechanism and role of such anions in the $LiFePO_4$ crystal structure are still not clear.

Similar to the controversy of supervalent cation doping, there are still many debates about whether these anions are actually doped into the $LiFePO_4$ crystal lattice, whether the increased performance of $LiFePO_4$ is due to the presence of carbon, and whether the anion-substitution in $LiFePO_4$ will affect the stability of PO_4 polyanions. For the time being, there is still no convincing evidence or answers for these questions.

Recent work by Chiang's group showed that doping can reduce the lithium miscibility gap as stated by Armand–Goodenough in 1997 for modified olivine,[15] ease phase transformation and expand Li diffusion channels.[69] However, given that Li site doping contributes much more to the increase of electronic conductivity than Fe site doping,[70,71] Li site doping may affect the activation energy of Li ion transportation and block the one-dimensional Li ion migration path,[72,73] which restrict the wide use of this technique in $LiFePO_4$. Up to now, to alleviate the poor electronic conductivity problem, the carbon coating technique is therefore still generally introduced to prepare C/$LiFePO_4$ composites.

3.4 Surface engineering of chemical composition

Another interesting report was published recently in *Nature* by G. Ceder's group concerning surface modifications by using

non-stoichiometric composition generating lithium phosphate species containing iron.[74] They achieved a rate capability equivalent to full battery discharge in 10–20 s under ambient temperature. The phenomenon was explained by a fast ion-conducting polyphosphate surface phase which increases lithium ion diffusion across the surface towards the (010) facet of $LiFePO_4$ and thus enhances the rate capability. However, the hypothesis was commented by J. B. Goodenough *et al.*,[75] and the debate still continues,[76] since it is difficult to discriminate between the impact of nano-sized particles in the presence of carbon coating on powder and the exact contribution of an additional lithium phosphate phase.

Other non-carbon second phase (*e.g.* metal oxides, polymers) coatings were also reported to modify the $LiFePO_4$ surface. Metal oxide has been used to improve the performance of $LiFePO_4$. V_2O_3 possesses a very high electronic conductivity of over 10^3 S cm^{-1} at room temperature, thus it was used as the second phase to modify C/$LiFePO_4$ to enhance its conductivity.[77] It was also found that some other metal oxides (CeO_2, ZrO_2, TiO_2) can not only enhance the discharge capacity but also improve the thermal stability and cycle performance.[78,79] The improved cycling performance is due to the metal oxide layer working as a protecting layer against HF attack from the electrolyte.[80] However, similar to metal additives, the uniform coating and high cost of metal oxides are still big challenges for its real application. By using the atomic layer deposition (ALD) technique, ultra-thin and uniform metal oxide films have been achieved in our recent work.[81,82] Dramatic electrochemical performance improvement has been demonstrated with only 2 atomic layers of Al_2O_3 on $LiCoO_2$ by other researchers.[83,84] ALD is therefore believed to be an important technique for surface coatings on $LiFePO_4$.[80]

Various approaches that have been attempted to improve the electrochemical performance of $LiFePO_4$ are illustrated in Table 1.

4. Understanding of carbon coating on $LiFePO_4$

4.1 Synthesis of $LiFePO_4$

Various synthetic methods have been explored to produce $LiFePO_4$ powder and have been reviewed in many review articles.[17,42,85] It is not the subject of this work to revisit all the synthetic methods, but we will instead discuss the synthetic methods in connection with carbon coating.

Generally speaking, all solid state or wet processes that have been reported so far for inorganic synthesis were used to make $LiFePO_4$, such as solid state reaction starting from all kinds of solid or liquid precursors[86–88] or wet chemistry processes including hydrothermal,[89] solvothermal,[90] ion-thermal,[91] sol–gel,[92] coprecipitation,[93] or spray pyrolysis.[94]

In the solid state reaction, carbon or carbon precursors are normally mixed with iron, phosphorus (or phosphate) and lithium sources. After reaction at an elevated temperature, $LiFePO_4$ is formed with carbon deposition on the particle surface. Mechanochemical activation has been reported to increase the reaction kinetics and lead to fine particles.[88]

Compared with the solid-state-based methods, the solution-based methods allow the precursors at the molecular level in solution to be homogeneously mixed. The carbon precursor may be incorporated into the precursors depending on the needs. For instance, in the sol–gel process, carbon precursors are usually added or be part of the chelating agent.[92] In this case, only $LiFePO_4$ precursor is formed at low temperatures during sol-gel process, and a further annealing process at higher temperatures (above 600 °C) is still required to make $LiFePO_4$. Under these high temperatures conditions, carbon deposition on $LiFePO_4$ surface can effectively suppress particle growth.[55] On the other hand, in the hydrothermal or solvothermal process, $LiFePO_4$ nanoparticles can be formed under pressure in an autoclave at low temperature (<200 °C). The particle size and morphology can be tailored by the pH, temperature and surfactant. In this case, normally carbon precursors are not necessarily be added. However, a post-treatment of the $LiFePO_4$ nanoparticles with organic precursors and calcination at elevated temperature are usually performed to increase the conduction. Details of carbon coating associated with each process will be discussed in Section 4.5.

4.2 Carbon addition to enhance the conductivity of $LiFePO_4$

To sustain fast charge and discharge in the battery, it is essential to have fast transport of electrons and lithium ions. In the commercial process of battery manufacturing, highly conductive carbon additives like carbon black, graphite or carbon fibers are often added to active materials with a binder to enhance the conductivity of the composite cathode or anode coating. When the particle size of $LiFePO_4$ becomes small (down to the nano or submicron size), a large proportion of carbon additive is required to connect all active materials, which causes low loading of active materials. Effective dispersion of carbon additives with active $LiFePO_4$ is also a challenge. Mechanofusion technology has been used to dry coating carbon nanoparticles on the $LiFePO_4$ surface. Surfactant addition to the coating slurry was also commonly used to help disperse carbon particles.

Carbon can also be added to the active materials during the synthesis process to improve the conductivity of the active materials. Various trials to add carbon particles to the reaction precursors have been made in the solid state and wet processes. The advantage is that one can add highly conductive carbon like graphite in combination with high surface area conductive carbon black. The challenge is to disperse the carbon well with the precursors. Usually a significant percentage of carbon (5–20 wt%) is required to reach the percolation point of high conductivity especially with submicron $LiFePO_4$ particles.[53]

The most effective way to increase the conductivity with a minimal dead weight penalty is to apply a carbon coating on the $LiFePO_4$ particle surface by pyrolysing solid-, liquid- or gas-phase organic precursors or a thin layer of polymers on the $LiFePO_4$ surface, as reported by Ravet *et al.*[50,51,54–56] In such a process a Pyrolytic Carbon Deposit (PCD) can be formed simultaneously during $LiFePO_4$ synthesis or after the synthesis in a second step. For instance, the pristine $LiFePO_4$ or its precursor can be coated with organic or polymeric materials in solution and then be heated to an elevated temperature to carbonize the organic layer forming a thin layer of carbon.

The poor conductivity can be improved by creating such a conductive carbon coating layer, sometimes at the nano-scale,

Table 1 Various approaches to improve the electrochemical performance of $LiFePO_4$.

Methods	Catalogue	Advantages	Disadvantages	Performance	References
Size reduction	Micro (10 μm)	High tap density	Low rate performance	C/LFP exhibits a specific capacity of 71 mA h·g^{-1} at 1 C	59
	Sub-micro (0.5–1.0 μm)	Medium tap density	Medium performance	C/LFP exhibits a specific capacity of 129 mA h·g^{-1} at 1 C	59
	Sub-micro (0.5μm)	Medium tap density	Medium performance	C-free LFP has a poor specific capacity of 72 mA h·g^{-1} at 1 C	60
	Nano-size (100–200 nm)	High rate performance	Low tap density	C-free LFP exhibits a capacity of 147 mA h·g^{-1} at 5 C	61
	Nano-size (20 nm)	High rate performance	Low tap density	C-free LFP exhibits a specific capacity of 163 mA h·g^{-1} at 1 C	62
Conductive surface coating	Metal (Cu/Ag)	High conductivity	High cost non-uniform	Cu or Ag (1 wt%)-$LiFePO_4$ exhibits a capacity of (140 mA h·g^{-1} at 0.2 C rate)	45
	Polymer (PPy/PANI)[a]	High conductivity	Poor mechanical properties	C/LFP/16 wt% PPy and C/LFP/7 wt% PANI exhibit a specific capacity of ~145 and ~140 mA h·g^{-1} at 1 C respectively	48
	Carbon	High conductivity	No improving intrinsic conductivity	Phostech C/LFP (0.5–1.0 μm) has a capacity of 150 mA h·g^{-1}	49
Lattice engineering	Supervalent cation doping	—	No convincing evidences	$Li_{1-X}M_xFePO_4$ (M = Zr, Nb, Mg) increases its conductivity by a factor of ~10^8 and has a capacity of ~150 mA h·g^{-1} at 0.1 C	63
	Anion doping	—	Possible structure change	$LiFe(PO_4)_{1-X}Cl_{3X}$/C ($x = 0.02$) delivered 138 mA h·g^{-1} at 1 C $LiFe(PO_4)_{0.9}F_{0.3}$/C shows 110 mA h·g^{-1} at 10 C	67,68
Surface engineering	Ion-conducting polyphosphate	—	Mechanism debates	$LiFe_{0.9}P_{0.95}O_{4-\delta}$ shows a super high capacity of 170 (20 C) and 130 mA h·g^{-1} (50 C)	74
	Metal oxide coating	Improving cycle performance	High cost, non-uniform	ZrO_2/LFP exhibits 146 mA h·g^{-1} at 0.1 C	77
				V_2O_3/LFP exhibits 143.5 mA h·g^{-1} at 0.2 C	78
				TiO_2 and CeO_2 improve the stability of LFP	79

[a] PPy: polypyrrole, PANI: polyaniline.

on the $LiFePO_4$ particles with a minimal amount of adherent carbon (usually less that 2 wt%).[50,51,55,56] The electrons can be spread to the entire surface of the particles through this carbon layer during charge/discharge and therefore improves the kinetics and reversibility of the lithium insertion/de-insertion cycles. This method of carbon coating can also suppress particle growth during or after synthesis and improve product purity by eliminating any Fe^{3+} species using the reducing gases generated from the pyrolysis.[55,95,96] These will be further discussed in the following sections.

4.3 Effect of carbon on the tap density of C/$LiFePO_4$

While carbon coating improves the conductivity of $LiFePO_4$, a monotonic decrease of tap density with carbon content is observed. This is understandable since carbon has much lower specific density than $LiFePO_4$ without taking into account possible carbon deposit porosity.[97] Chang *et al.* investigated the effect of carbon content on the tap density of $LiFePO_4$ synthesized using self-produced high-density $FePO_4$ as a precursor,[98] and glucose as a carbon source, and found that the tap density

decreases from 2.15 to 1.66 g cm^{-3} when the carbon content increases from 3 wt% to 9 wt%. An optimum carbon content of 7 wt% was suggested, which gives a tap density of 1.80 g cm^{-3}, and a superior electrochemical performance than other compositions. Clearly, the 7% of carbon is dead mass, leading to 7% capacity loss, which is not efficient for developing high-performance commercial materials.

Tap density of C/$LiFePO_4$ is not only determined by the carbon content, but also determined by the particle size, particle morphology and particle size distribution. A spherical C/$LiFePO_4$ material synthesized by using the precipitation method gave a tap density of 1.75 g cm^{-3},[99] which is remarkably higher than the non-spherical $LiFePO_4$ powders (tap-density 1.0–1.3 g cm^{-3}) of similar size. Another method being reported recently to improve C/$LiFePO_4$ tap density is to prepare agglomerate particles. For example, a tap density of 1.1 g cm^{-3} was achieved by preparing agglomerate C/$LiFePO_4$ composite *via* the spark-plasma-sintering (SPS) technique.[100] More recently, further improvement has been reported by using a two-step drying method to increase the tap densities from 1.37 to 1.80 g cm^{-3}.[97] This improvement could be attributable to the net structure formed by adding a second drying step in the process, resulting in agglomerations of the colloid particles. Because of the denser structure, the grains of the particles are more prone to grow and crystallize in the drying process. Another report shows that composite synthesized with two kinds of Fe^{3+} precursors (consisting of nanometre-sized and micrometre-sized particles) exhibited less vacancy than that prepared with single Fe^{3+} precursor (composed mainly of micrometre-sized particles) and led to high tap density which increases from 1.19 to 1.40 g cm^{-3} (Fig. 5).[101]

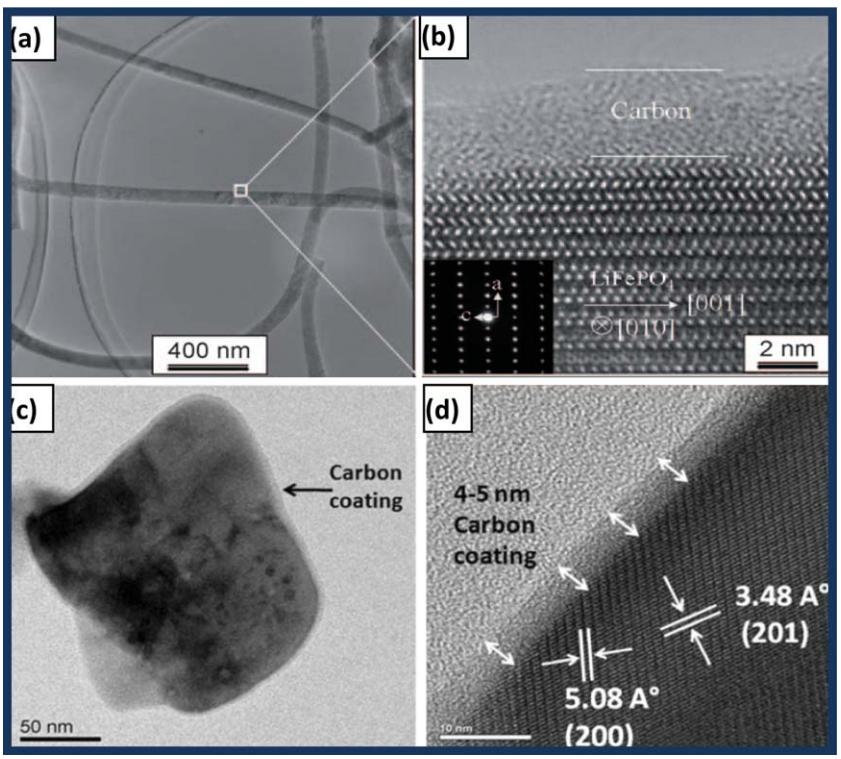

Fig. 4 (a) TEM image and (b) high-resolution TEM image of single-crystalline C/$LiFePO_4$ nanowires (reproduced with the permission from ref. 57, Copyright 2011 Wiley), (c) TEM image and (d) high-resolution TEM image of C/$LiFePO_4$ nanoplate (reproduced from ref. 58 with permission; Copyright Springer 2010).

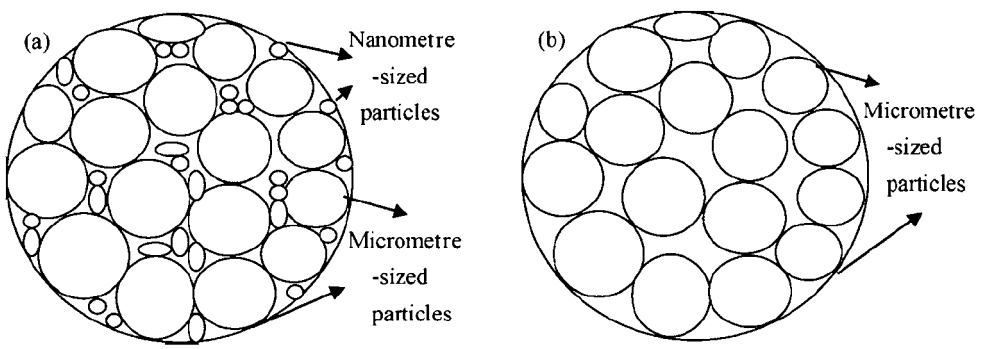

Fig. 5 The possible packing models of the samples (a) LFP1 and (b) LFP2. Reprinted from ref. 101 with permission. Copyright 2010 Elsevier.

In addition, tap density of the C/$LiFePO_4$ is well related to the experimental conditions and methods. The calcination temperature in the coprecipitation method is an important influencing factor for tap density of C/$LiFePO_4$ as it affects the morphology and crystal structure of the powders.[102] Sun *et al.* reported that C/$LiFePO_4$ prepared at 800 °C exhibited high crystallinity as well as a higher tap density of 1.09 g cm^{-3} compared with the one prepared with other temperatures (650, 700, 750, and 850 °C). In further work, the tap density of C/$LiFePO_4$ (~3 wt% carbon amount) was increased to 1.5 g cm^{-3} by using self-prepared $FePO_4$ as precursor and a pitch as carbon source.[103] This highly dense C/$LiFePO_4$ material consisting of nanoscale particles (200–300 nm) and pores (100–200 nm) shows a 2.5 times greater volumetric energy density with similar rate capability compared with nano $LiFePO_4$. More recently, to improve the uniformity of carbon coating combining with high tap density,[104] they reported a double carbon coating on microscale nanoporous $LiFePO_4$. Carbon coated $FePO_4$ was first prepared *via* coprecipitation using sucrose as the first carbon source, and the resulting C/$FePO_4$ was further mixed with Li_2CO_3 (lithium source) and pitch (the second carbon source) and calcined at high temperature (Fig. 6). This material still has a high tap density of 1.5 g cm^{-3} with about 0.5 wt% carbon amount and a superior specific capacity, rate capacity, and volumetric energy density. Meanwhile, in another work, to make better dispersion of carbon on $LiFePO_4$ through the coating of its precursor, polyvinylpyrrolidone (PVP) was also employed as the carbon source to reduce the polarity of water and a smooth and homogeneous carbon precursor coating was achieved on micro-scale $LiFePO_4$.[105] The 6 μm C/$LiFePO_4$ microsphere with a higher tap density (1.6 g cm^{-3}) exhibits an excellent rate capability and delivers a volumetric capacity of 225 mA h cm^{-3}.

4.4 Effect of carbon on the properties of C/$LiFePO_4$ composite

Carbon coatings greatly enhance the specific capacity, rate capacity and cycling performance of $LiFePO_4$. Cyclic voltammetry (CV) was used to evaluate the kinetics of lithium intercalation and de-intercalation.[50,52,106] Each of the CV curves consists of an oxidation peak and a reduction peak, corresponding to the charge–discharge reaction of the Fe^{2+}/Fe^{3+} redox couple. The midpoint between the oxidation and reduction peaks, which corresponds to the redox potential of the $LiFePO_4$ electrode, is about 3.45 *vs.* Li/Li^+. In pure $LiFePO_4$ materials without carbon coating, a larger separation between redox peaks appears, indicating a reduced reversible behavior which is mainly related to the sluggish diffusion step. Coating olivine particles with a carbon layer can greatly improve reversible performance for the insertion and extraction of Li ions and their kinetics. This is because the pyrolytic carbon in the product suppresses sintering and particle growth during or after synthesis, leading to fine particles which shorten the distance of the transport passages in the solid-phase, and improves the insertion and extraction of Li ions. The separation potential between redox peaks was also reduced further with the increasing content of carbon.[98,106] The peak current of C/$LiFePO_4$ nanocomposite materials increases with carbon content also, which means better electrode reaction kinetics and better rate performance of the $LiFePO_4$ cathode material.

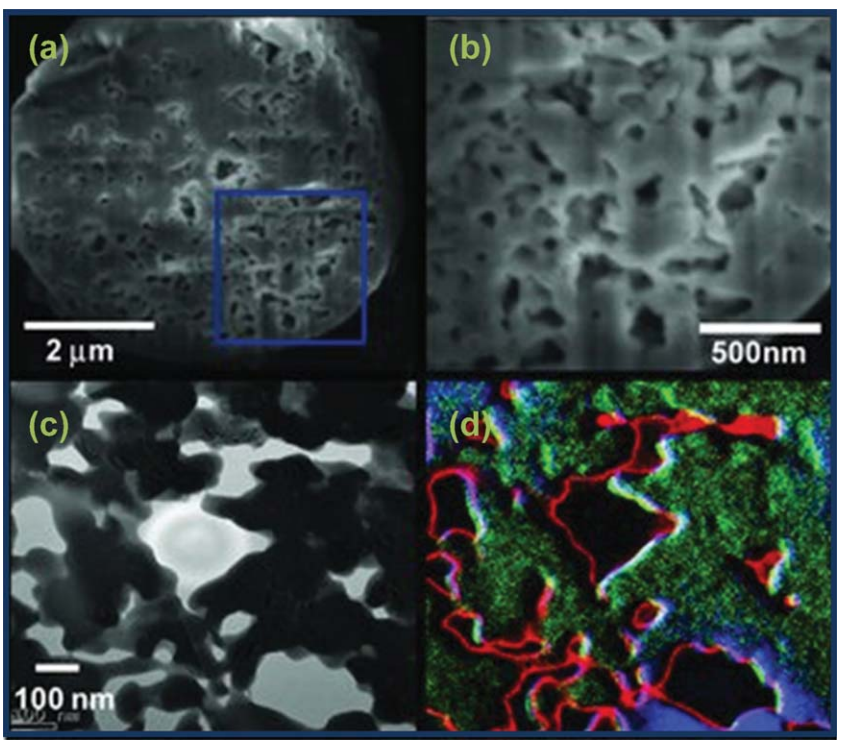

Fig. 6 SEM images obtained from a focused ion beam cut of $LiFePO_4$ at low (a) and high (b) magnification. Cross-sectional TEM image of $LiFePO_4$ (c) and the corresponding EELS image (d) (where red: C, blue: Fe, and green: P). Reprinted from ref. 104 with permission. Copyright 2010 Wiley.

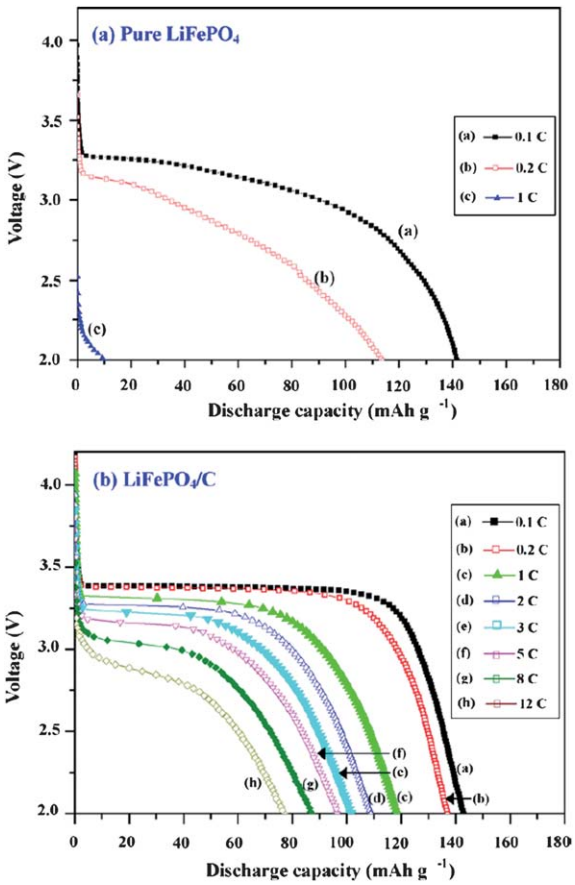

Fig. 7 The typical charge and discharge curves of (a) $LiFePO_4$ (pure) and (b) $LiFePO_4$/C cells. Reprinted from ref. 107 with permission. Copyright 2008 Elsevier.

Great improvement of specific capacity can be achieved on $LiFePO_4$ after carbon coating, which is due to the better reversible performance for Li ion insertion and extraction and the electrode kinetics (Fig. 7).[107,108] A high conductivity as a result of the carbon coating can also lead to a reduction of the cell impedance (Fig. 8).[109] A further decrease of the charge transfer resistance can be obtained with the increase of carbon content. Thus the rate capacity of $LiFePO_4$ can be greatly enhanced by carbon coating.[107,110]

Besides the better specific capacity and rate performance, better cycling performance of $LiFePO_4$ can be obtained by carbon coatings. A good cycle performance of less than 5% discharge capacity loss over 1100 cycles at a low discharge rate (0.6 C rate) was reported in a C/$LiFePO_4$ nanocomposite with a core–shell structure.[111] The cycling stability of C/$LiFePO_4$ at a high discharge rate is very critical for practical applications. A recent report reveals that the C/$LiFePO_4$ composite also shows a greatly enhanced cyclic stability at 4 C, which is retained as high as 92% after 1000 cycles.[112] In another report,[113] $LiFePO_4$/carbon composite was synthesized by a simple high-energy ball milling combined with the spray-drying method, the C/$LiFePO_4$ composite obtained shows a greatly enhanced rate performance and an excellent cyclic stability at room temperature with 92% retention of its original discharge capacity beyond 2400 cycles (10 C rate). In addition, the cycling performance was affected by the synthesis conditions,[114] although the material synthesized at a lower sintering temperature had higher discharge capacity due to a lower degree of crystallization and plenty of nano-sized microstructure. The lower sintering temperature also leads to the instability of the crystal structure and the solution of active materials, which results in the degradation of discharge capacity over long-time cycling. Therefore, synthesizing the material with

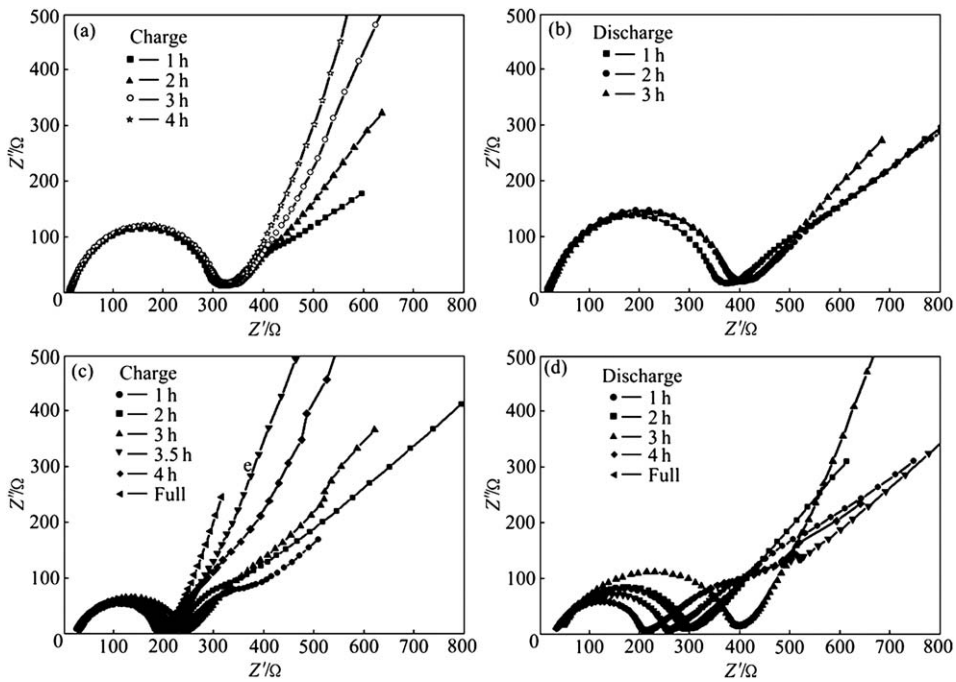

Fig. 8 Electrochemical impedance spectra of cathodes: (a) Non-modified $LiFePO_4$; (b) non-modified $LiFePO_4$; (c) CNTs-modified $LiFePO_4$; and (d) CNTs-modified $LiFePO_4$. Reprinted from ref. 109 with permission. Copyright 2010 Elsevier.

high crystallization and moderate particle size in the presence of the carbon source is an effective way to improve the cycling performance of C/$LiFePO_4$ cathode materials.

In this section, the details of carbon coating including carbon sources, carbon content, carbon thickness, carbon structure, carbon distribution and morphology, and carbon surface area and porosity are reviewed.

4.4.1 Carbon content and carbon coating thickness. Carbon coating on $LiFePO_4$ improves utilization of the active material, which results from the reduction of the grain size[115,116] and the improvement of electrical conductivity.[50] However, carbon has an adverse effect on the tap density.[116] A large amount of carbon will decrease the volumetric energy density of C/$LiFePO_4$ composites more severely than the gravimetric energy density. Therefore, it is important to find the optimum content of conductive additive which affects the utilization of active material and the energy density of the electrode.

However, it is difficult to define the optimum carbon content without discussing the carbon structure, the carbon distribution, morphology as well as the $LiFePO_4$ effective surface developed, especially with nano-scale particles. If the carbon is not homogeneously distributed on the $LiFePO_4$ particle surfaces, as in most cases, it is even harder to define the optimum amount of carbon content (wt%) and carbon film thickness. The carbon film thickness is generally related to the carbon content, and high carbon content can generally contribute to high conductivity but also means thick carbon coating (for instance larger than 3–5 nm) which might restrict the easy penetration of lithium ions. Less carbon means thin carbon coating, low negative impact on tap density, but it is normally linked with non-uniform coatings or not enough surface conductivity.

Zaghib *et al.* investigated the electrochemical properties of $LiFePO_4$ cathodes containing different carbon contents from 0 to 12% of conductive additive (carbon black or a mixture of carbon black and graphite) and found that the specific capacity increases with increasing carbon content and does not show a maximum value until 12% of carbon content,[117] but it does show decreased volumetric capacity of electrode. Another study reported an optimum range of carbon content from 3.5 to 10.3%, and the performance rapidly decreased with further increase in the carbon content.[118] The rapid decrease of performance can be attributed to the following possible reasons: (1) amorphous carbon phase dilutes the density of the crystalline $LiFePO_4$ phase, (2) excess carbon suppresses formation of the crystalline $LiFePO_4$ phase, and (3) high carbon content combined with high temperature (800 °C) reduces Fe and P to form inactive Fe_2P. Compared with the range of carbon amount, an exact optimum 5 wt% was reported which shows a best performance of C/$LiFePO_4$ in a battery.[119] A similar optimum carbon content (4.6%) was also reported using a different preparation method.[120] However, the optimum carbon content is different in various studies. Lu *et al.* added high surface area carbon to $LiFePO_4$ and indicated that C/$LiFePO_4$ with 8.0 wt% carbon exhibited the best performance.[121] Chang *et al.* suggested that 7 wt% carbon may be an optimum value for the C/$LiFePO_4$ material with regard to the tap density because the greater carbon content will result in the lower tap density,[122] but the discharge capacity increases little if the carbon content is over 7 wt%.

The optimum value reported for carbon content varies in the literature. This is because the synthesis process including precursors, experimental conditions and methods strongly influences the physical characteristics of the formed carbon material, resulting in the different electrochemical behavior of C/$LiFePO_4$ materials. For example, 90% of the theoretical capacity at the 0.5 C rate in C/$LiFePO_4$ composites at room temperature has been achieved by using 15 wt% carbon gels as a carbon source.[53] The same capacity value was obtained by reducing the carbon content to nearly 3 wt% in other reports using a different carbon incorporation method.[116] Thus the optimum carbon content can be just considered as a reference value in these studies since in fact total carbon in the electrode has to be taken into account which contains the carbon coating, other particulate carbon introduced during $LiFePO_4$ synthesis, and any other carbon added to the binder during the composite electrode formulation. Considering the impact of carbon on tap density and volumetric capacity, a lower carbon content is critical for real applications. A small amount of *in situ* carbon (~1.5 wt%) derived from ethylene glycol was reported to decrease the particle size of $LiFePO_4$ and to improve significantly the rate capability of $LiFePO_4$.[123,124] The obtained C/$LiFePO_4$ material shows a high-rate capacity with 150 mA h g^{-1} at C/25 rate and around 100 mA h g^{-1} at 5 C rate. Although the capacity is not the highest one among the reported studies, the lowest carbon content reported in the literature makes it more promising in industrial production and application.

During the carbon coating process, the carbon is usually derived from organic precursors that are added to the reaction mixture before firing. During firing, the organic material is decomposed and carbonized in an inert or reducing atmosphere. Therefore, carbon thickness also can be controlled by the addition of the amount of carbon precursors. It is easily understood that the carbon coating thickness increases with the amount of carbon precursor. For example, a carbon coating thickness of about 1–2 nm was obtained by Dominko *et al.* from 3.2 wt% citrate anion as a carbon source, while it increased to about 10 nm when 12.3 wt% citrate anion was used (Fig. 9).[125] In addition, although there are no reports showing direct evidence for the relationship between carbon thickness and carbon precursor, it is not difficult to understand this correlation because different carbon precursors have various optimum decomposed temperatures and contribute to different amounts of carbon which generally lead to different carbon thickness. Moreover, carbon thickness is also related to the $LiFePO_4$ particle size and surface area. Smaller-sized $LiFePO_4$ particles with higher surface areas generally get thinner carbon layers when carbon amount and physical properties are fixed because more surface area is coated due to the high surface area of small-sized $LiFePO_4$.

With regard to the effect of carbon thickness on the C/$LiFePO_4$ performance, Cho *et al.* indicated that the thickness of carbon and conductivity increases with the carbon content.[126] By controlling the thickness of carbon (from a few nanometres to a few tens of nanometres where the carbon content was controlled between 1.25 and 2.54 wt%), the sample with the carbon thickness of 4–8 nm exhibited the best discharge capacity due to the easy diffusion of lithium ion and uniform coatings. It is evident that an optimum carbon coating thickness is desirable to balance the conductivity and easy lithium ion penetration, but

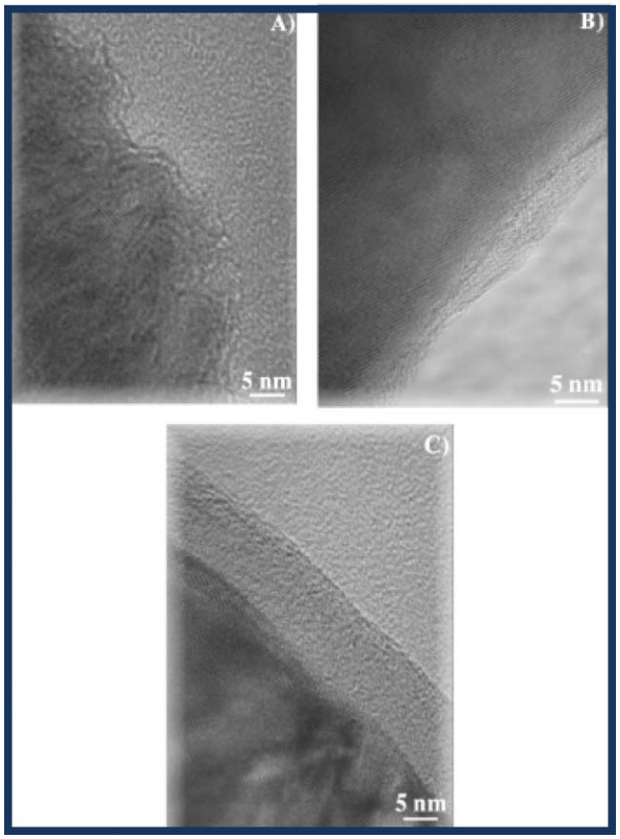

Fig. 9 HRTEM images of tiny edges of $LiFePO_4$/C composite particles. (A) Crystal planes in the [200] direction are ending in about 1 nm thick carbon layer (the source of carbon was solely the citrate anion), (B) crystal planes in the [101] direction are ending in about 2–3 nm thick carbon layer (the source of carbon was citrate anion and 1.7 wt% of HEC) and (C) crystal planes in the [211] direction are ending in about 10 nm thick carbon layer (the sources of carbon were citrate anion and 20.4 wt% of HEC). Reprinted from ref. 125 with permission. Copyright 2005 The Electrochemical Society.

similar to the optimum carbon amount, it is also difficult to find an identical value among different studies. For example, core–shell C/$LiFePO_4$ composites synthesized *via* a chemical vapor deposition assisted solid-state reaction show 3 nm carbon coating, which exhibits a high specific capacity of 114.6 mA h g^{-1} at 5 C rate.[127]

Because the synthesis method and precursors used vary in different reports in the literature, it is meaningless to compare these optimum carbon content values and thicknesses directly. However, from the aforementioned studies, it is obvious that a thin carbon film with low carbon content is important for $LiFePO_4$ in order to have easy diffusion of lithium ion and high tap density. However, it is still a challenge to make thin and uniform carbon coatings on $LiFePO_4$.

4.4.2 Carbon structure. The structure of the carbon coated on the surface of the $LiFePO_4$ particles significantly affects the electrochemical performance of C/$LiFePO_4$.[128] The extent of graphitized carbon and its ratio to the disordered carbon is usually characterized by the I_D/I_G (disordered/graphite) ratio in the Raman microprobe spectrum.[129,130] The lower D/G ratio is an indication of the higher amount of graphitized carbon. It is reported that C/$LiFePO_4$ with low I_D/I_G ratios outperformed those with a higher amount of carbon having a more disordered structure.[131] It is clear that the high amount of graphitized carbon is more desirable in view of its contribution to the electronic conductivity of the cathode material (the electrical conductivity of graphite and acetylene black are 6.4×10^{-2} and 5.7×10^{-4} S cm^{-1}, respectively[132]). Therefore, how to effectively control the carbon structure during the synthesis process is very critical for high performance C/$LiFePO_4$.

The structure of the carbon deposit can be tuned by using additives during C/$LiFePO_4$ synthesis. The choice of an appropriate carbon source can directly affect the carbon structure. A high amount of graphite carbon is observed for the C/$LiFePO_4$ composite prepared with sucrose as an additional source of carbon.[133] The incorporation of naphthalenetetracarboxylic dianhydride during synthesis also results in a more graphitic carbon coating and improves utilization of $LiFePO_4$ in lithium cells.[129] Besides, the addition of a small amount of functionalized aromatic or ring-forming compounds before the final heating process also enriches graphitized carbon in the residual carbon.[128,129,134,135] Recently, a polyaromatic compound, *e.g.* polystyrene, with a lower sp^3/sp^2 peak ratio contributes to more highly graphite-like carbon formation for $LiFePO_4$ during polymer pyrolysis and the resultant C/$LiFePO_4$ exhibited a superior capacity.[136]

Although optimizing the carbon structure can be achieved by choosing an appropriate carbon precursor, it is still difficult to produce highly graphitic coatings by the pyrolysis at relatively low temperatures (600–800 °C) used for synthesis of $LiFePO_4$ because carbon is difficult to graphitize at these low temperatures without catalysts. It is well known that some iron compounds can catalyze the formation of graphite at relatively low temperatures. Raman studies indicate that such an effect can occur at a pyrolysis temperature of 700 °C, which is much lower than the pyrolysis process without catalysts.[95,96]

Furthermore, carbon nanotubes, which consist of curled graphene sheets, can be made at temperatures as low as 600–700 °C using organic or polymeric carbon sources and iron compounds as catalysts. Thus, addition of graphitization catalysts during the preparation process may result in carbon with lower D/G ratios or more graphite carbon material. Doeff *et al.* realized it by adding small amounts of ferrocene (graphitization catalysts) into pyromellitic acid (carbon sources),[131] and the C/$LiFePO_4$ material obtained shows dramatically improved rate performance even with an overall carbon content of below 2 wt%.

Apart from carbon sources, the preparation method has an important impact on the formation of carbon structure. Similar to carbon nanotube growth, a novel chemical vapor deposition (CVD) assisted solid-state route was reported that a graphite shell with the thickness of 3–5 nm was formed on $LiFePO_4$ using polyvinyl alcohol (PVA) and benzene vapor as the reducing agent and carbon source (Fig. 10).[127] The discharge capacity of C/$LiFePO_4$ with a graphite shell is much higher than that of the $LiFePO_4$ composite without a graphite shell. Such a chemical vapor deposition-assisted synthesis method may be more promising for synthesis of C/$LiFePO_4$ composite material.

Another way to increase the graphite carbon content is by direct addition of highly graphitic carbon material to $LiFePO_4$.

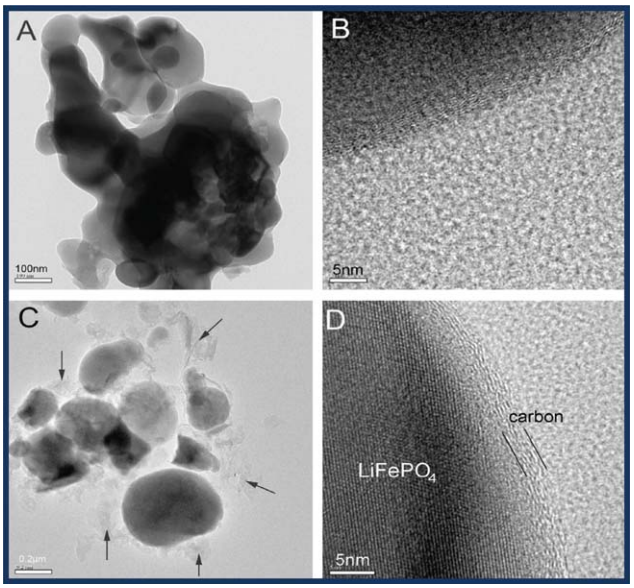

Fig. 10 TEM micrographs of C/$LiFePO_4$ composites (A and B) without CVD and (C and D) with CVD. Reprinted from ref. 127 with permission. Copyright 2009 Elsevier.

Carbon nanotube is a promising material due to the highly graphite content and superior conductivity.[137,138] Liu *et al.* investigated the effect of carbon nanotubes on the electrochemical performance of $LiFePO_4$ batteries.[139] Compared with the $LiFePO_4$ batteries with carbon black additive, those with carbon nanotube additive show better electrochemical performance with a capacity retention ratio of 99.2% after 50 cycles at 1/3 C rate. This is because the carbon nanotubes functioned as a link to connect the $LiFePO_4$ particles and enabled active materials to transport lithium ions and electrons at fast rates, resulting in the disappearance of Li-ion migration resistance through the SEI film and the decrease of charge transfer resistance (Fig. 11).[107,140–143] Besides carbon nanotubes, Carbon Nano-Fibers (CNFs) have been used in replacement of amorphous carbon.[144] The addition of functionalized Carbon Nano-Fiber to $LiFePO_4$ also shows better electrochemical performance compared to the addition of acetylene black to $LiFePO_4$, even though the coating is not homogeneous. The improved performance is probably due to the high electronic conductivity of the cathode material due to the CNF addition and the efficient contact between electrochemical active particles and the electronic conducting CNFs.

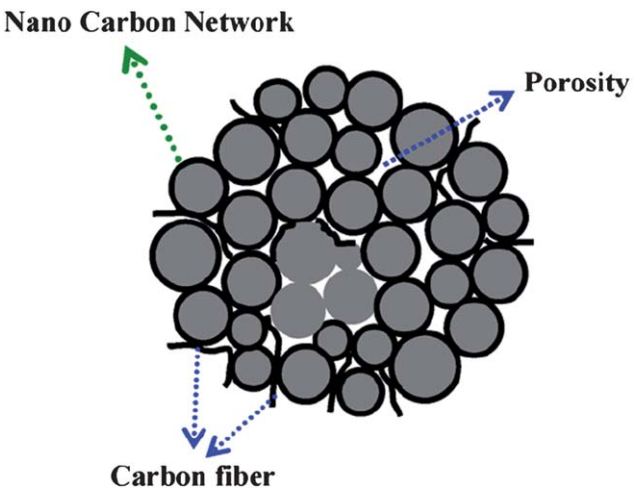

Fig. 11 The schematic representation of $LiFePO_4$/C powders with a continuous nanocarbon network. Reprinted from ref. 107 with permission. Copyright 2008 Elsevier.

Recently, as a novel carbon material, graphene has shown its great potential in $LiFePO_4$ applications due to its unique structure, superior electronic conductivity, and high surface area. Su *et al.* directly mixed graphene with a commercial $LiFePO_4$ material to form the graphene-based conductive network. The conducting network was constructed flexibly through a "plane-to-point" mode due to the soft two-dimensional structure of graphene, compared to the "point to point" conducting mode in the conventional carbon-based conductive additive.[145] The obtained $LiFePO_4$/graphene composite exhibits an excellent electrochemical performance. In addition to direct mixture, more studies were performed by introducing graphene during the $LiFePO_4$ synthesis process. Ding *et al.* prepared $LiFePO_4$/graphene composites by a coprecipitation method and achieved considerable improvement in capacity delivery and cycle performance of $LiFePO_4$.[146] However, the rate performance was not significantly improved because $LiFePO_4$ nanoparticles were only loosely loaded on graphene sheets and limit the enhancement in electronic conductivity. Zhou *et al.* recently wrapped $LiFePO_4$ nanoparticles with a 3D graphene network and formed spherical graphene-modified $LiFePO_4$ by spray-drying and annealing processes.[147] The conductive network can facilitate electron transport effectively, while the presence of abundant voids between the $LiFePO_4$ nanoparticles and graphene sheets was beneficial for Li^+ diffusion. The composite cathode material thus delivers a superior rate performance of 70 mA h g^{-1} at 60 C discharge rate. The effective three-dimensional conducting network with bridging graphene nanosheets was also created by a hydrothermal route in another report.[148] Consequently, graphene may offer great potential for applications in future high-performance $LiFePO_4$.

4.4.3 Carbon morphology and distribution. In view of the one-dimensional Li ion mobility in the framework, full carbon coverage ensures $LiFePO_4$ particles transfer electrons along all directions during charge and discharge. It was postulated that an ideal structure for high-performance $LiFePO_4$ should contain nano-sized particles completely coated with conductive carbon. The ultimate goal in many studies is to find a simple and efficient method for synthesis of $LiFePO_4$ with uniform carbon coatings.

There are mainly two methods for carbon introduction to $LiFePO_4$. One is direct addition of various particulate carbon materials by mechanical means, which allows the choice of high surface area carbon or high-graphitized carbon material, but no available techniques can lead to uniform coating on the surface of $LiFePO_4$ since carbon is neither soluble nor fusible. The other method is *in situ* deposition by using the pyrolysis of a carbon precursor during the synthesis of $LiFePO_4$, which allows the achievement of uniform coating of the precursor on $LiFePO_4$. Kim *et al.* compared C/$LiFePO_4$ composite materials with two different carbon addition methods.[149] One is carbon powder direct introduction and the other is using sucrose as the carbon

precursor. The sucrose precursor method leads to the formation of a thin, porous and more uniform carbon coating around the particles and results in a slightly higher discharge capacity compared to the other sample.

In spite of this, these approaches based on the thermal decomposition of carbon-containing precursors can still only produce $LiFePO_4$ particles with a partial coating of carbon. A uniform carbon coating is still highly desirable. Recently, an *in situ* polymerization method was developed by Wang *et al.* for the synthesis of a C/$LiFePO_4$ composite formed from a highly crystalline $LiFePO_4$ core with a size of about 20–40 nm and a uniform semi-graphitic carbon shell with a thickness of about 1–2 nm (Fig. 12).[111] Aniline was oxidization polymerized on the outer surface of $FePO_4$ with the presence of Fe^{3+} and then Fe^{3+} ions were reduced to Fe^{2+} during the process. After the subsequent heat treatment, the polymer shell was transformed into a carbon shell that restricts the *in situ* crystallite growth of $LiFePO_4$.

Although much work has been done to form a uniform film of carbon on $LiFePO_4$, it is still a major challenge to achieve homogeneously uniform carbon coverage especially on irregular shaped particles and agglomerates, which are more difficult to cover completely and would require more carbon than spherical ones. In view of that, introduction of $LiFePO_4$ into a carbon network and matrix may be a compromised method and has attracted some interest.[107,150–153] A continuous, dispersive nano-carbon network was reported by Chen and demonstrated high rate capability (≥12 C) and long cycle life (≥700 cycles at a 3 C discharge rate).[107] The use of a nanoporous carbon matrix serves as a mixed conducting 3D nano-network, enabling both Li ions and electrons to migrate and reach each active particle, hence realizing the full potential of nanoactive materials. Wu embedded $LiFePO_4$ nanoparticles in a nanoporous carbon matrix.[152] In this nanocomposite, the electronically conducting nanoporous carbon matrix with mesopores filled by electrolyte can be considered not only as a mixed conducting 3D network that allows both Li ion and electron to migrate and reach each $LiFePO_4$ nanoparticle, but also as an electrolyte container for high rate charging/discharging. The nanocomposite electrode shows a superior high power/energy capability. Sides *et al.* designed a new type of template-prepared nanostructured $LiFePO_4$ electrode consisting of monodispersed nanofibers of the $LiFePO_4$ electrode material mixed with an electronically conductive carbon matrix.[153] This unique nanocomposite morphology allows these electrodes to have a capacity of 150 mA h g^{-1} at a rate of 5 C and maintains a substantial fraction of the theoretical capacity even at rates exceeding 50 C. This new nanocomposite electrode shows such excellent rate capabilities because the nanofiber morphology mitigates the problem of slow Li ion transport in the solid

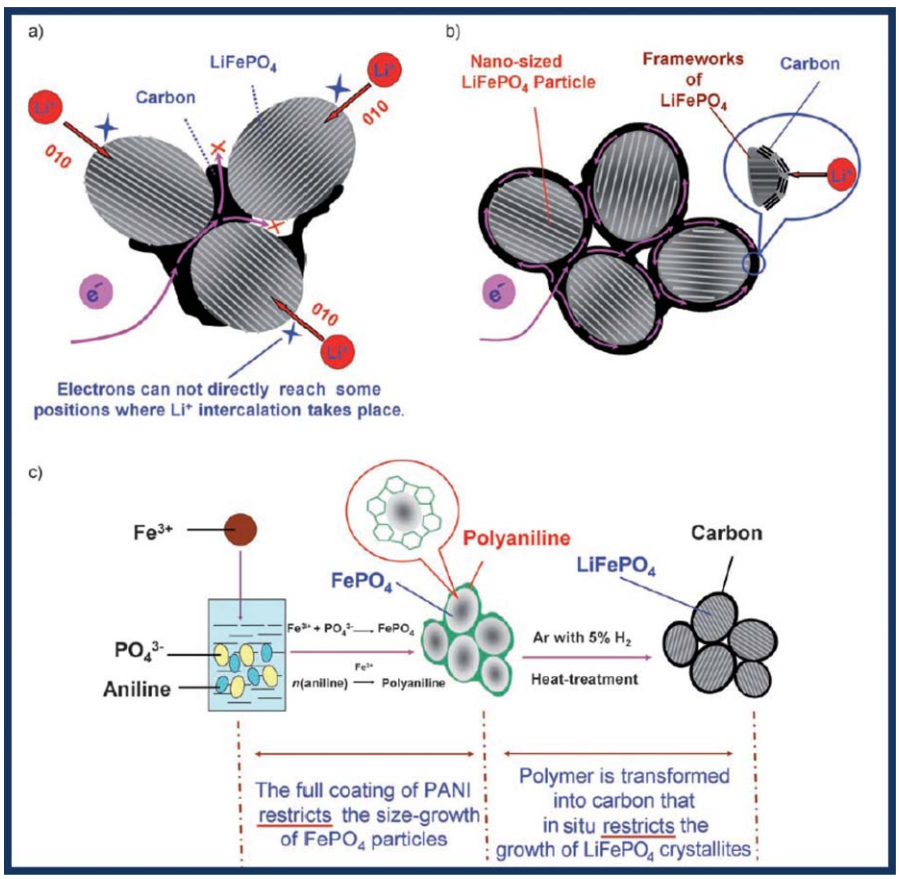

Fig. 12 (a) Electron-transfer pathway for $LiFePO_4$ particles partially coated with carbon. (b) Designed ideal structure for $LiFePO_4$ particles with typical nano-size and a complete carbon coating. (c) Preparation process for the C/$LiFePO_4$ composite including an *in situ* polymerization reaction and two typical restriction processes. Reproduced from ref. 111 with permission. Copyright 2008 Wiley.

state, and the conductive carbon matrix overcomes the inherently poor electronic conductivity of $LiFePO_4$.

4.4.4 Carbon surface area and porosity. It is believed that a carbon layer with high surface area and porous network structure plays an important role in improving the electrochemical properties of $LiFePO_4$,[154] which can be attributed to the following reasons: (i) a porous carbon network structure serves as electrolyte containers to provide multi-dimensional channels for diffusion of lithium ions and to shorten enormously the diffusive distance of lithium ions, resulting in a high rate charge/discharge rate; (ii) the porous network structure of carbon layer has a large specific surface area, which could provide large active sites for lithium ions' intercalation/deintercalation into/from $LiFePO_4$ nanoparticles; and (iii) the porous structure of carbon with high surface area would prohibit the expansion of particles during heating.

Lu *et al.* studied $LiFePO_4$ cathode material coated with high surface area carbon (BET surface area, 2099 $m^2\ g^{-1}$) by the pyrolysis of peanut shells under argon and treatment with a proprietary porogenic agent,[111] with the goal of altering the pore structure and increasing the surface area of the pyrolysis carbon. The high surface area carbon increases the overall conductivity of $C/LiFePO_4$ composite from 10^{-8} to 10^{-4} S cm^{-1} and increases the specific area of the composite resulting in improved electrochemical performance including specific capacity, cycling properties and rate capability.

The introduction of hydrolyzed sugar gives a porous carbon structure on $LiFePO_4$ because the sugar ($C_{12}H_{22}O_{11}$) is hydrolyzed to glucose ($C_6H_{12}O_6$) and fructose ($C_6H_{12}O_6$), which ultimately oxidizes to gluconic acid or a polyhydroxyl acid. The polyhydroxyl similar to polymer has cross-link property, which would decompose to porous structure of carbon. The resultant $LiFePO_4/C$ composite can achieve high specific capacity (143 mA h g^{-1}) after the 100 cycles with 1 C charge/discharge rate at 50 °C.[155] Wang *et al.* reported that the decomposition of polyethylene glycol led to a porous structure of carbon on $LiFePO_4$.[156] The satisfactory initial discharge capacity (139 mA h g^{-1} at 1 C) and superior rate capacity therefore can be obtained. Recently, the yeast cells as a template and cementation agent and glucose as carbon source is adopted to prepare the porous carbon coated $LiFePO_4$ composite.[157] The $C/LiFePO_4$, with the specific surface area of 98.3 $m^2\ g^{-1}$, exhibits an initial discharge capacity of 147 mA h g^{-1} and superior cycling stability.

Along with carbon sources, preparation methods also affect the surface area and porosity. The sol–gel method based on citric acid is a widely used method to prepare porous $C/LiFePO_4$ composite materials.[158,159] Perfectly interconnected pores are formed due to vigorous gas evolution (mainly CO and CO_2) during degradation of a citrate precursor. The superposition of a continuous thin carbon film (electron conductor) on pores (ion conductor when filled with electrolyte) represents a unique architecture in which the electrons and ions are simultaneously supplied to the site of insertion in the particle interior. Superior electrochemical performance may be obtained while preserving a high tap density.

4.4.5 Carbon sources. Among various organic precursors for carbon coating, sucrose and glucose are the most popular ones. Numerous studies have been conducted on the synthesis of high-performance $C/LiFePO_4$ composite by applying them as the carbon sources.[160–162] An appropriate calcination condition is critical for the performance of the final product using sucrose as carbon sources. Insufficient calcination temperature or time could result in the residual CH_x remaining in the electrode and lead to a decrease of electrode performance.[160] Compared with sucrose, glucose was found to be a better candidate. Chen *et al.* compared the $C/LiFePO_4$ being synthesized by using sucrose and glucose as the carbon sources and found that the $C/LiFePO_4$ composite prepared with glucose as the carbon source exhibited higher initial discharge capacities.[161] At discharge rates of 0.1 C, the initial discharge capacities were 133.3 and 155.0 mA h g^{-1} for $LiFePO_4$ with sucrose and glucose as the carbon sources respectively. Lai also achieved an excellent rate performance and a good cycling stability for $C/LiFePO_4$ using glucose as well as carbon sol–gel as the carbon sources.[162]

Organic carboxylic acids are also a common carbon source. Citric acid may be the most popular carboxylic acid for carbon sources and has attracted much interest due to the low pyrolysis temperature (as low as 450 °C).[163] This feature ensures a low synthesis temperature of $C/LiFePO_4$ composite with a high surface area and a small particle size. Zhang *et al.* synthesized $C/LiFePO_4$ by using citric acid as a carbon source and showed high discharge capacities of ~153 and 92 mA h g^{-1} at 1 C and 20 C rates respectively.[164] Yan *et al.* also reported a superior performance of $C/LiFePO_4$ synthesized by a solid-state reaction using citric acid as a carbon source.[163] It delivers an initial discharge capacity of 128 mA h g^{-1} at 4 C, which is retained as high as 92% after 1000 cycles. In addition, at −20 °C, the composite exhibits a discharge capacity of 110 mA h g^{-1} at 0.1 C. In addition to citric acid, Fey attempted to coat $LiFePO_4$ by incorporating various organic carboxylic acids as carbon sources.[165,166] These acids include: (a) mono-acid containing a ring structure (salicylic acid, malonic acid), (b) straight-chain diacids (sebacic acid, adipic acid, ascorbic acid), and (c) tri-acids (citric acid). The use of carboxylic acid as a carbon source increases the overall conductivity (~10^{-4} S cm^{-1}) of the material. The best cell performance was delivered by the sample coated with 1.9 wt% carbon using 60 wt% malonic acid as the carbon source.

In addition to sugar and organic carboxylic acids, various polymeric precursors were also studied. It was found that highly graphitized carbons are formed during pyrolysis of functionalized aromatic or ring-forming compounds on $LiFePO_4$.[166,167] A polyaromatic compound, *e.g.* polystyrene, with more functionalized aromatic groups displayed improved performance because its decomposition temperature was close to the temperature of the $LiFePO_4$ phase transformation, which resulted in fine particle size and uniform carbon distribution on the composite surface.[168]

4.4.6 Highly conductive impurity phase formation. During the synthesis process of $LiFePO_4$ material, some conductive metal phosphides (FeP, and metallic Fe_2P) may be produced, which was first reported by Nazar's group. They suggested that this metal phosphide acts as the actual electronic conductor for Zr-doped $LiFePO_4$.[169] In their further work,[170] it was reported that the conductive iron phosphides were generated on the parent $LiFePO_4$ by *in situ* reaction of $LiFePO_4$ with carbon under reducing gases. FeP and Fe_2P are found to be thermodynamically

stable at 600 and 800 °C respectively. Under the mildest reducing conditions, FeP is formed on the surface along with Li_3PO_4. Under more aggressive reducing conditions, FeP is still present, but thermodynamics favor the formation of Fe_2P. The transformation from FeP to Fe_2P can be achieved by the vaporization of phosphorus above 600 °C.[171] The metallic Fe_2P phase is present in between the $LiFePO_4$ and carbon coating. Nazar *et al.* also showed that these $LiFePO_4$-Fe_2P "composites" gave significantly enhanced electrochemical rate properties as well as outstanding cyclability.[169]

At room temperature, the conductive Fe_2P has an electronic conductivity of 1.5 S cm^{-1}, whereas the semiconducting amorphous carbon formed at the intermediate processing temperatures (typically, 600–750 °C) displays conductivity on the order of 10^{-3} S cm^{-1}.[169,170] It is believed that iron phosphides play a more important role in improvement of the bulk conductivity of $LiFePO_4$. Xu *et al.* also indicated that the carbon amount, morphology, and particle size are directly related to the formation of Fe_2P.[172] This Fe_2P phase among the C/$LiFePO_4$ composite increases the electronic conductivity and evidently improves the electrochemical performance of the composite, whereas too much iron phosphides will lower the discharge capacity of the electrode since they are inert for the de-insertion/insertion of lithium ion.[173] Therefore, an optimum amount of iron phosphides may be important for C/$LiFePO_4$ with high performance. In practical preparation processes, the coating carbon can also be considered as the reductive additive under high temperature with Ar gas, and the presence of this reducing circumstance may promote the formation of these highly conductive iron phosphides, all of which should be considered in synthesis of high-performance C/$LiFePO_4$ composite.

4.5 Synthesis process to control carbon coating of C-$LiFePO_4$ composites

4.5.1 Ex-situ carbon coating on already synthesized $LiFePO_4$. Carbon can be coated or introduced on previously synthesized $LiFePO_4$ as a post-synthesis treatment. One of the advantages of this method is that one can synthesize highly pure $LiFePO_4$ prior to carbon coating to enhance the purity of the composite material. The other advantage is choosing various formed carbon materials especially graphitized carbon to improve carbon quality, but the uniform carbon coating is often a big challenge.

It is well known that an inherent difficulty in the conventional solid-state process for synthesis of $LiFePO_4$ is achieving a homogeneous mixture of the precursors. Trivalent ions in the precursors have extremely low diffusion coefficients in the solid state. Thus, it is hard to avoid parallel reactions and inhomogeneities. Some impurity phases therefore appear and by-products remain. To cope with it, melt casting provides us a promising method to make highly pure $LiFePO_4$. Instead of the conventional solid-state process, synthesis in the molten state is an ideal liquid-phase reaction, so high purity and high tap density for the material can be expected. However, one usually can get ingot or large particles by atomization and further grinding to micron and nano-size is needed, which can be achieved by various milling technologies.

In a typical synthesis process, a variety of "low cost" precursors will be melted at 1000 °C followed by cooling leading to a high purity $LiFePO_4$ material with excellent crystallinity and large crystals. The phase purity, crystallinity, and microstructures of the final product depend on the reducing conditions and the solidification process of the melt. Particle size reduction of the resulting $LiFePO_4$ ingot was achieved by a continuous wet milling procedure, which reduces the particle size of the $LiFePO_4$ crystals to 200 nm. C/$LiFePO_4$ samples were prepared by pyrolyzing a variety of carbon precursors to $LiFePO_4$ at 700 °C. Applying carbon coating of the $LiFePO_4$ particles made by melt casting/grinding shows some similarity to that of hydrothermal particles and clear differences are high crystallinity and high purity as well as simplicity of the process. In addition, Zhou *et al.* also synthesized well-crystallized $LiFePO_4$ by the KCl molten salt method.[175] Sucrose was used as a conductive precursor and contributed to 3 wt% carbon in the final product. The obtained C/$LiFePO_4$ composite has a high tap density of 1.55 g cm^{-3} and shows good electrochemical activity.

4.5.2 *In situ* carbon coating during the $LiFePO_4$ synthesis process

Solid-state reaction based methods. Solid-state synthesis is a conventional method for preparing C/$LiFePO_4$ which includes several successive steps of intimate grinding and annealing of the stoichiometric mixture of starting materials. In a typical synthesis process, the starting materials containing lithium sources, phosphorus source, and iron(II) precursors were first pretreated at low temperature to prepare precursors and then crystallized at high temperature under an inert or reducing atmosphere to prevent oxidization of iron(II).

Temperature is an important factor influencing the synthesis process of C/$LiFePO_4$. Impurities and an ill-defined crystalline structure are often found in the final products if the sintering temperature is low. However, large particle size and broad particle size distribution of $LiFePO_4$ powder are usually obtained in a solid-state method due to the high sintering temperature. Therefore, there is an optimum temperature for solid-state synthesis of carbon coated $LiFePO_4$ for every different precursor combination.[176–178] Zhang *et al.* reported that the optimized temperature was 800 °C,[176] and the capacity of the $LiFePO_4$ was decreased as the temperature was higher or lower than 800 °C. This is because high temperature induces growth and sintering of $LiFePO_4$ particles. However, most of other researchers used a lower temperature ranging from 600 °C to 700 °C to get smaller-sized products. In addition to its impact on particle size, temperature also affects the shape of the grains. An obvious anisotropic growth occurred at a high temperature and the growth rate along the (100) crystal plane was more rapid than that of (111) crystal.[179] However, the anisotropic growth of the grain is restrained at 650 °C and spherical carbon-coated $LiFePO_4$ was obtained, which had excellent electrochemical performance.

Conventional solid state methods use iron(II) precursors as starting materials, which increase the preparation cost of the $LiFePO_4$/C composite. In a variant of these conventional solid-state method, Fe(III) salts can be used as raw materials in the presence of a reductant, reducing the material cost and simplifying the manufacturing process. As a reductant, pure carbon can be added directly during the carbothermal reduction process to make C/$LiFePO_4$.[180] Organic carbon precursors can also serve

as the reductants during the pyrolysis process to reduce the Fe^{3+} precursor ($FePO_4 \cdot 2H_2O$),[51,54,56] which will also combine the carbon coating process and reducing process and a reduction process from hydrogen containing pyrolysis gases in one step.[95,96] An advantage of this combined process is to benefit from the pyrolytic carbon deposit and a low reduction temperature to better control $LiFePO_4$ sintering and particle growth.[55] A comparison between pure carbon (acetylene black) and carbon precursor (glucose) as carbon sources has been made and the C/$LiFePO_4$ synthesized using glucose as carbon source showed a higher electrochemical capacity and the lower capacity fading,[181] which is due to a uniform carbon coating on $LiFePO_4$ through *in situ* pyrolysis of the glucose precursor.[182]

Temperature still significantly affects the morphologies and performance of synthesized C/$LiFePO_4$ composites in conventional solid-state and carbothermal processes. Both the crystallization degree and particle size increase remarkably with the synthesis temperature.[183] The material synthesized at lower sintering temperature had lower crystallization degree and plenty of nano-sized particles, leading to its high electrochemical activity and high initial discharge capacity. However, the lower sintering temperature also leads to the instability of the crystal structure and the solution of active materials, which results in the degradation of discharge capacity on long-time cycling. Thus, synthesizing the material with perfect crystallization degree and moderate particle size at an optimum temperature in a reduction process is very important to improve the cycling performance of C/$LiFePO_4$.

Although the solid-state reaction with or without reduction has been widely adopted for synthesis of crystalline olivine-phase $LiFePO_4$, it is a complex process, including in some cases repeated grinding to gain homogeneous particles and several steps at high temperature to impede formation of the impurity phase. These repeated heating treatments result in undesirable particle growth and agglomeration, presenting a major drawback to practical implementation of this synthesis method.

Recently, the microwave irradiation method has been proposed for the preparation of many functional materials due to its prominent advantages such as heating the material at the molecular level, uniformity, low cost and especially shorter reaction time. Thus, a product with small and uniform particle size can easily be obtained due to the uniform heating and avoiding long reaction time at high temperatures. Zhan *et al.* developed a rapid synthesis method of highly crystalline C/$LiFePO_4$ composite by microwave heating in under 4 min with glucose as the carbon source and reducing agent.[184] Compared with the pure solid-state method, the sample obtained with ball-milling followed by microwave irradiation method has a smaller average particle size (160–600 nm) and more uniform size distribution due to the rapid reaction. Cycling tests show that the sample prepared by a microwave method can deliver 150 mA h g^{-1} at 17 mA g^{-1} (0.1 C).

Wet chemical methods. In comparison with conventional solid-state reaction methods, solution-based methods offer advantages of homogeneous mixture of precursors at the molecular level which ensure higher phase purity of $LiFePO_4$ and low reaction temperature to better control of particle size and morphology such as small size and porous structure achieved *via* a sol–gel method.[185] The material prepared with the sol–gel process usually exhibits a better electrochemical rate performance due to a larger number of surface apertures, a smaller mesoporous volume, and a more interlaced pore system compared with the solid-state method. The sol–gel method also offers a wide choice of carbon sources like citric acid,[186] sucrose,[187] lauric acid,[188] ethylene glycol,[189] and polymer.[190] Yang and Xu synthesized a C/$LiFePO_4$ composite of a particle size of 200–300 nm by a sol–gel method.[191] The composite demonstrated specific capacities of around 150 mA h g^{-1} at discharge rates of 2 C. A smaller size of 20–30 nm C/$LiFePO_4$ composite was achieved by a sol–gel process using citric acid as a complexing agent and a carbon source.[192] The electronic conductivity of the nano-sized C/$LiFePO_4$ composites is greatly improved, reaching a value of 2.46 $\times$ 10^{-3} S cm^{-1} at room temperature. Furthermore, the rate capability of the synthesized C/$LiFePO_4$ composite is much improved because of its small grain size and good electronic conductivity compared with other studies.

In addition to the sol–gel method, the hydrothermal (or solvothermal) method is also one of the common wet chemical methods for *in situ* preparation of C/$LiFePO_4$ composite. By assistance with the microwave technique, the hydrothermal process can be finished within a few minutes, which provides a rapid, one-spot method for synthesis of C/$LiFePO_4$. Manthiram *et al.* synthesized the C/$LiFePO_4$ nanocomposite *via* a microwave-assisted hydrothermal method and the material has a more uniform particle size (220–225 nm) and exhibits high capacity with excellent cyclability and rate capability.[193] They also compared the microwave-assisted hydrothermal (employing water as a solvent) and solvothermal (employing tetraethyleneglycol as a solvent) synthesis approach and found that the microwave solvothermal process employing a tetraethyleneglycol as a solvent offers much smaller particle size than the microwave-hydrothermal process employing water as a solvent (Fig. 13).[194] Thus, microwave-solvothermal methods may be more promising for synthesis of high performance C/$LiFePO_4$.

Gas state method-spray pyrolysis. It is well known that the electrochemical performance of the electrode is strongly affected by the powder properties, such as the mean size, the morphology, the specific surface area, the crystallinity, and the composition of the material.[195] Spray pyrolysis is thought to be an effective technique for producing cathode powders with fine size and regular morphology as well as high crystallinity and phase purity.[196–198] Even if the post-annealing of as-prepared powders is required to obtain the desired materials, a shorter annealing time of the as-prepared powders can be expected in comparison with conventional solid-state preparation methods. In contrast, several long sintering and regrinding procedures are sometimes needed to obtain the final product in the conventional solid-state reaction method, resulting in a severe increase of particle size.

Kang *et al.* prepared carbon-mixed $LiFePO_4$ by spray pyrolysis from a colloidal spray solution.[199] The nano-sized material affected the morphologies, mean particle sizes, and electrochemical properties of the $LiFePO_4$ cathode powders. Micro-sized $LiFePO_4$ powder with narrow size distributions can be obtained and carbon coating improved the initial discharge capacity and the cycle performance of the $LiFePO_4$ powders. The similar micro-sized carbon included $LiFePO_4$ powders also

prepared by spray pyrolysis from the spray solution with sucrose.[200,201] However, the electrochemical performance of the above-prepared materials was not sufficient for large-scale application because the size of the $LiFePO_4$ particles was submicron or micron-sized.[202] By a combination of spray pyrolysis with wet ball-milling, $LiFePO_4$ nanoparticles with a mean diameter of 58 nm were successfully prepared.[202,203] The sample delivered a superior performance with the first discharge capacities of 100 mA h g^{-1} at charge–discharge rates of 10 C.

Recently, ultrasonic spray pyrolysis has been shown to be an effective technique for producing fine ceramic particles with homogeneous chemical composition in a short time.[204] With the assistance of an ultrasonic technique, the precursors were dispersed and mixed more homogeneously. The purity of the products is higher, and the composition of the powders is easy to control. Moreover, non-agglomerated powders were obtained. Therefore, ultrasonic and ball-milling assisted spray pyrolysis are attractive methods for fabrication of high-density samples because in these methods well-crystallized and homogeneous small particles can be prepared with the spherical shape and pure phase.

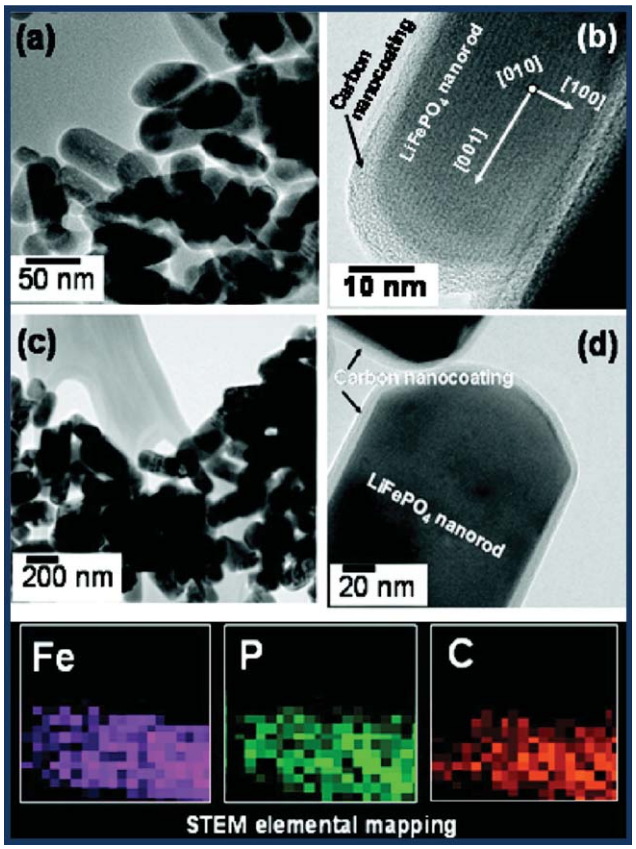

Fig. 13 (a) TEM and (b) high resolution TEM images of the $LiFePO_4$/C nanocomposite obtained by an *ex situ* carbon coating of the MW-ST $LiFePO_4$ nanorods by heating with sucrose at 700 °C for 1 h in a flowing 2% H_2/98% Ar atmosphere. (c) TEM and (d) high resolution TEM images of the $LiFePO_4$/C nanocomposite obtained by an *in situ* carbon coating with glucose during the MW-HT process, followed by heating at 700 °C for 1 h in a flowing 2% H_2/98% Ar atmosphere. Reproduced from ref. 194 with permission. Copyright 2008 American Chemical Society.

More details about the effects of the synthesis process and the coated carbon on the performance of C/$LiFePO_4$ are summarized in Table 2.

4.6 Thin-film electrode technique for interface and mechanism study

Carbon coating techniques on $LiFePO_4$ have been developed and commercialized. However, the role of carbon is still not completely understood in spite of its importance in the rate capability and cycle stability of $LiFePO_4$ electrodes. Geometrically, well-defined thin films are suitable for fundamental research since there are no binder and conductive additives included.[205] This is especially true for poorly conductive active materials because the thickness can be reduced to a value at which the poor electronic conductivity does not significantly affect the electrochemical behavior. Therefore, the intrinsic properties of $LiFePO_4$ can be investigated by using the carbon-free thin film. Nowadays, various techniques have been used to prepare $LiFePO_4$ thin films, *i.e.*, pulsed laser deposition (PLD),[206–208] radio-frequency magnetron sputtering deposition (RF-MSD),[209,210] and electrostatic spray deposition.[211] Among them, PLD and RF-MSD are the more common methods for preparation of $LiFePO_4$ thin film electrodes. Chung employed the pulse laser deposition technique to deposit the C/$LiFePO_4$ composite thin films on the $Si/SiO_2/Ti/Pt$ substrates (Fig. 14).[212] The effects of carbon content and post-deposition annealing treatments on the electrochemical performances of the as-deposited film electrodes were carefully investigated. The results showed that the co-deposited carbon was homogeneously distributed throughout the $LiFePO_4$ films and 2 mol% carbon was the optimized amount for the highest capacity.

Thin film technology was also of particular interest to provide insights on the mechanism study. Li-ion diffusion kinetics was studied by Xie in detail,[213] who prepared $LiFePO_4$ thin films using radio frequency (RF) magnetron sputtering. The Li-ion diffusion kinetics has proved to be affected by the incorporation of carbon.[214] Compared with the C/$LiFePO_4$-binder composite electrodes, thin film electrodes seem to be more appropriate for the measurement of the chemical diffusion coefficient since they are conducting additive and binder free, and have a well-defined geometry and good contact with the current collector.

In addition to the help in understanding the carbon coating process and mechanism, $LiFePO_4$ thin film electrodes with thickness ranging from a few nanometres to hundreds of nanometres are also essential for solid-state microbatteries, especially in low power applications, as the active or standby power sources for microelectronics. It has been demonstrated that $LiFePO_4$ thin films can be used as a promising cathode film for lithium microbatteries by depositing the $LiFePO_4$ film with RF-MSD.[215] Similarly, C/$LiFePO_4$ thin films with a thickness of 1 μm were also deposited on a stainless steel substrate by RF-MSD.[210] The presence of carbon enhances the electronic conductivity, resulting in a high rate capability.

Thin film technology (with no conducting additive) has thus thrown some light on the intrinsic sensing properties of $LiFePO_4$ thin films as well as provided insights on their sensing response mechanism. Of most importance, the role of carbon may be investigated in detail by coating a thin carbon film on the

Table 2 The effect of carbon on the performance of the C/$LiFePO_4$ composite material

Preparation method	Carbon				Electrochemical performance	References
	Precursors	Content	Thickness	Structure (I_D/I_G)		
Solid-state reaction	Citric acid	—	—	0.53	Initial discharge capacity of 128 mA h g^{-1} (4 C) and was retained as high as 92% after 1000 cycles	112
Solid-state reaction	Benzene	—	3 nm	0.75–0.77	Initial discharge capacity of 155.4 (0.1 C) and 135.8 mA h g^{-1} (1 C)	127
Solid-state reaction	Peanut shells	0, 6, 8, 10, 12 wt%	—	0.928–0.962	LFP[a] (8.0 wt% carbon) exhibits an initial discharge of 138 and 128 mA h g^{-1} at (0.2 C) after 170 cycles	121
Solid-state reaction	Glucose	3,5,7,9 wt%	—	—	LFP (7 wt% carbon) has discharge capacity of 167.0 mA h g^{-1} (0.1 C) and 98.3 mA h g^{-1} (5 C)	69
Solid-state reaction	PS[b] + malonic acid	0.02–2.54 wt%	2–25 nm	~0.95	LFP (2.28 wt% carbon, 4–8 nm) delivers maximum discharge capacity of 151 mA h g^{-1} (0.2 C) and sustains 415 cycles at 80% of capacity retention	19
Coprecipitation	PEO[c], PS, PB[d] and SBS[e]	~2 wt%	—	0.99–1.14	PS sample delivers the largest charge capacity of 147 mA h g^{-1} at 0.5 C	136
Sol–gel	Acetylene black, sucrose and glucose	5–30 wt%	—	—	Initial discharge capacity was 125.3 (acetylene black), 133.3 (sucrose) and 155.0 (glucose) mA h g^{-1} at 0.1 C	161
Sol–gel	Citrate	3.2–12.7 wt%	1–10 nm	—	LFP (3.2 wt%, 1–2 nm carbon thickness) exhibits best performance of 150 mA h g^{-1} (0.2 C) and 117 mA h g^{-1} (5 C)	125
Sol–gel	Citric acid, sucrose	—	2.4–4 nm	1.5	Discharge capacities of 153, 120, 112, and 94 mA h g^{-1} at 0.1, 1, 3, and 5 C rates, respectively	133
Microwave	Glucose	0, 2.8, 7.4, 12.1, 17.2 wt%	—	—	LFP (12.1% carbon) exhibits the best discharge capacity of 147 mA h g^{-1} and good cycling stability (more than 141 mA h g^{-1} at the 20th cycle) at 0.1 C	157
Hydrothermal	Carbon black	0, 3, 5, 10 wt%	—	—	LFP (5% carbon) was 128 mA h g^{-1} at 1st cycle and 127 mA h g^{-1} after 30 cycles (0.1 mA cm^{-2}), respectively	119
Microwave	Polyethylene glycol	3.9%, 4.6%, 5.2%, 7.3%	—	—	LFP (4.6% carbon) has a largest initial specific capacity of 152 mA h g^{-1} at 0.2 C	120
Solvothermal	Carbon nanotubes	8 wt%, 5.2%, 7.3%	—	—	LFP has discharge capacity of ~161 mA h g^{-1} (0.1 C) of 152 mA h g^{-1} (0.2 C) and 59 mA h g^{-1} (20 C)	151

[a] LFP: LiFePO4. [b] PS: polystyrene. [c] PEO: polyethylene oxide. [d] PB: polybutadiene. [e] SBS: styrene–butadiene–styrene.

$LiFePO_4$ film. Carbon features including carbon content, structure, thickness, *etc.* can be investigated accurately. By combining with material characterization techniques such as scanning electron microscopy (SEM), transmission electron microscopy (TEM), X-ray photoelectron spectroscopy (XPS), Raman, and synchrotron based *in situ* X-ray diffraction,[216–218] more detailed information about carbon and even the interface between carbon and $LiFePO_4$ film can be obtained, which will be very helpful for the development of high performance $LiFePO_4$.

5. Promising synthesis methods of C/$LiFePO_4$ for future large-scale production

For industrial applications, large-scale and high-quality C/$LiFePO_4$ combining with low processing cost and easy manufacturing are the primary requirements for the synthesis methods. Based on these factors, there are several promising methods for mass production including solid-state reaction, hydrothermal method, and molten state method (Table 3).

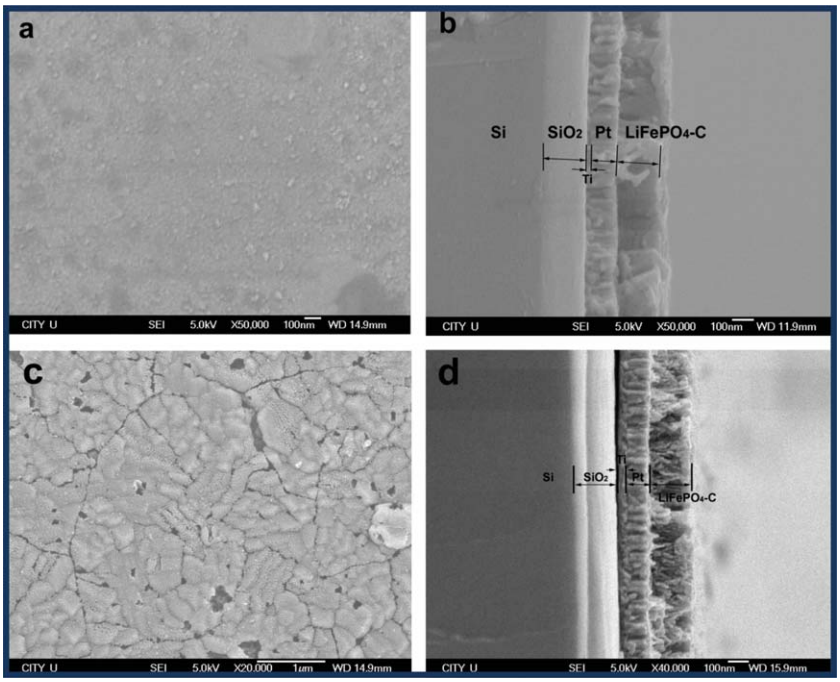

Fig. 14 (a and c) Plane-view and (b and d) cross-section SEM images of the $LiFePO_4$-C thin films. (a and b) Before and (c and d) after annealing treatment at 600 °C for 6 h. Reproduced from ref. 212 with permission. Copyright 2008 American Chemical Society.

As the conventional method for mass production of most lithium-ion battery cathode materials, the solid-state method is still the most widely used process for mass production of C/$LiFePO_4$ due to process simplicity in synthesis and carbon coating, in spite of the drawback of particle size control.

The hydrothermal/solvothermal methods have great potential for nano-sized C/$LiFePO_4$ in large-scale production. With the addition of carbon precursors, this method can prepare and manufacture high surface area C/$LiFePO_4$ powders with improved rate performance. The obtained C/$LiFePO_4$ products are more suitable for high power application. However, the challenges for hydrothermal/solvothermal methods are process complexity and high cost.

By combining the advantages of the solid-state reaction (high crystallinity) with the hydrothermal method (uniform chemical mixture and high-purity phase), the molten-state method provides a simple, reliable, cheap, less wasteful technique to produce high quality $LiFePO_4$ for large-scale battery applications. The synthesis within a molten state combines ideal liquid-phase reaction kinetics and short dwell times to provide a product with high material density using a simple process method. This simple synthetic method can use the various common precursors. The melting of carbon-coated $LiFePO_4$ powder at 1000 °C followed by its cooling leads to a high purity $LiFePO_4$ material with excellent crystallinity and large crystals. With the proper milling procedures, the melting products can be made into various sizes from micro-, sub-micro-, to nanosize. With the following pyrolytic carbon deposit process,[51] various-grade C/$LiFePO_4$ can be achieved to fulfil the needs of current and future battery markets (Fig. 15).[59,174] With the increasing demands for electric vehicles, a simple synthetic method using commodity precursors or even natural sources is required for the large-scale synthesis of $LiFePO_4$. It is believed that the molten synthetic method is a viable alternative to the current methods of synthesis.

Table 3 Promising synthesis methods of C/$LiFePO_4$ for future large-scale production[a]

Methods	Advantages	Disadvantages	Size	C addition	Grade	References
Solid-state based	Low cost, process simplicity	Difficult to control particle growth	Sub-micro or micro-size	*In situ* coating or post-addition	Energy	219,220
Hydrothermal method	Nanosize, morphology control (NPs, NWs, NRs, *etc.*)	Waste liquid. Strict reaction conditions (temperature, pH, time, *etc.*)	Nano-size	*In situ* coating or post-addition	Power	221,222,223
Molten state	Simplicity, low cost, common precursors, high crystallinity	No effective morphology controls	Nano-, sub-micro, micro-size	Post-addition (PCD process)	Both	59,174

[a] NPs: nanoparticles; NWs: nanowires; NRs: nanorods; PCD: Pyrolytic Carbon Deposit.

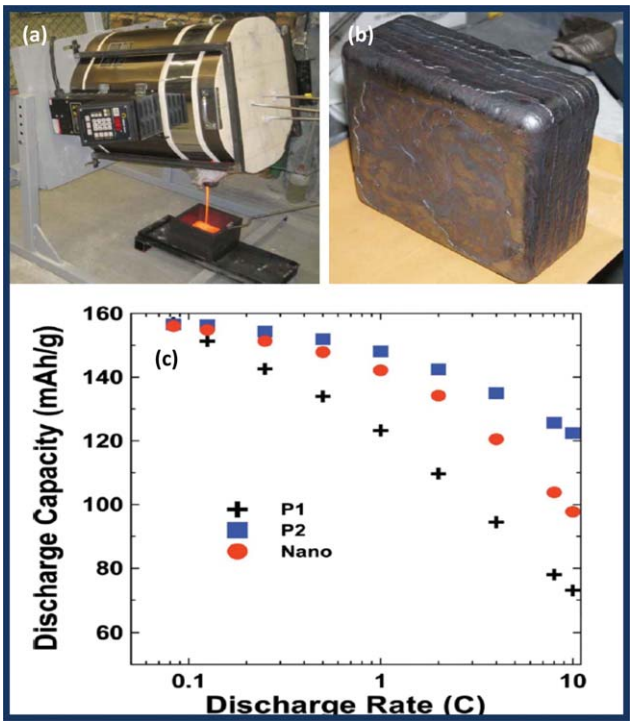

Fig. 15 (a and b) Photograph of large-scale $LiFePO_4$ casting from synthesis and the resultant 10 kg ingot in Phostech Lithium Inc. (c) Comparison of commercial energy grade $LiFePO_4$ (P1, cross), power grade $LiFePO_4$ (P2, squares), and nanomilled melt-cast $LiFePO_4$ samples (circles). Reproduced from ref. 59 and 174 with permission. Copyright 2010. The Electrochemical Society.

6. Conclusions and remarks

Although C/$LiFePO_4$ materials have been successfully commercialized and the contributions of carbon to $LiFePO_4$ in improving conductivity and rate capacity have been widely accepted, some fundamental questions still remain and need to be investigated in detail.

Uniform and full carbon coatings throughout the $LiFePO_4$ powder are an ideal structure, which ensures $LiFePO_4$ particles transfer electrons through all directions and alleviate the polarization phenomenon. Carbon coatings must also be either porous or very thin to allow easy penetration of lithium ions. Therefore, it is very important to seek a simple and efficient method for synthesis of $LiFePO_4$ with uniform carbon coatings.

Optimizing the carbon structure is the key to obtain good performance of $LiFePO_4$. While highly graphitic carbon material can greatly enhance the electrochemical behavior of $LiFePO_4$, it is difficult to produce highly graphitic coatings at relatively low temperatures used for synthesis of $LiFePO_4$. Direct introduction of carbon nanotubes or graphitic carbon or *in situ* growth of these graphite materials on $LiFePO_4$ will be an effective method. An in-depth study of the surface chemistry of $LiFePO_4$ and its influence on carbon coating will direct the optimization of the nature of the carbon coating.

A high tap density of C/$LiFePO_4$ material is considered to be an important factor for practical applications. The introduction of carbon, however, decreases the energy density of the material significantly, especially for the volumetric energy density. An effective route to improve the material's tap density is to design novel structures, including spherical, aggregated and especially microspheral structures composed of tightly compacted nanocrystallites.

The role of carbon is still not completely understood in spite of the fact that its importance in the rate capability and cycle stability of $LiFePO_4$ electrodes has been proven. Thin film electrodes are of great interest because they can serve as a simplified model for elaborating the detailed electrochemical process of their counterpart active materials. Carbon can be coated on the surface of $LiFePO_4$ thin-film electrodes and the details of carbon effect, lithium-ion penetration through carbon layer, and the interface between $LiFePO_4$ and carbon can be investigated to develop a better understanding.

With regard to the large-scale industrial production, a reliable, low-cost, highly effective synthetic method for C/$LiFePO_4$ is still highly desirable. The solid-state method has already been widely adopted by industry for mass production, and it will remain one of the most used processes for manufacturing C/$LiFePO_4$ due to process simplicity and low cost. The wet process including hydrothermal, solvothermal has great potential for nano-sized C/$LiFePO_4$ production because it can moderate the size and morphology of C/$LiFePO_4$. Although currently this method has some drawbacks such as strict reaction conditions, it is still a very promising synthetic approach for future power-grade cathode materials. Compared with the above two methods, the molten state method combines the advantages from solid-state reaction and hydrothermal methods and provides a simple, reliable, cheap, less wasteful technique to produce well defined $LiFePO_4$ for large-scale battery applications. With the proper procedures, the melting products can be made into various sizes from micro- to nano-size and fulfil various needs of energy-grade and power-grade products for current and future battery markets. This novel method might become a very competitive candidate for future C/$LiFePO_4$ production.

Acknowledgements

This work is supported by Natural Sciences and Engineering Research Council of Canada (NSERC), Phostech Lithium Inc., Canada Research Chair (CRC) Program, the University of Western Ontario, and MITACS Elevate Strategic Fellowship Program. The authors express their sincere thanks to Dr Michel Gauthier and Dr Guoxian Liang for the fruitful discussion on the organizing and drafting of this work. The authors are also in debt to David Tweddell and Dr Henry Huang for their kind help and discussion.

Notes and references

1 O. K. Park, Y. Cho, S. Lee, H.-C. Yoo, H.-K. Song and J. Cho, *Energy Environ. Sci.*, 2011, **4**, 1621–1633.
2 G. Jeong, Y.-U. Kim, H. Kim, Y.-J. Kim and H.-J. Sohn, *Energy Environ. Sci.*, 2011, **4**, 1986–2002.
3 B. Scrosati, J. Hassoun and Y.-K. Sun, *Energy Environ. Sci.*, 2011, **4**, 3287–3295.
4 V. Etacheri, R. Marom, R. Elazari, G. Salitra and D. Aurbach, *Energy Environ. Sci.*, 2011, **4**, 3243–3262.
5 X. Zhi, G. Liang, L. Wang, X. Qu, J. Zhang and J. Cui, *J. Power Sources*, 2009, **189**, 779–782.
6 M. S. Whittingham, *Chem. Rev.*, 2004, **104**, 4271–4302.

7 C. H. Chen, J. Liu, M. E. Stoll, G. Henriksen, D. R. Vissers and K. Amine, *J. Power Sources*, 2004, **128**, 278–285.
8 M. M. Thackeray, W. I. F. David, P. G. Bruce and J. B. Goodenough, *Mater. Res. Bull.*, 1983, **18**, 461–472.
9 J. B. Goodenough and Y. Kim, *Chem. Mater.*, 2010, **22**, 587–603.
10 P. P. Prosini, M. Lisi, D. Zane and M. Pasquali, *Solid State Ionics*, 2002, **148**, 45–51.
11 R. Amin, P. Balaya and J. Maier, *Electrochem. Solid-State Lett.*, 2007, **10**, A13–A16.
12 A. K. Padhi, K. S. Nanjundaswamy and J. B. Goodenough, *J. Electrochem. Soc.*, 1997, **144**, 1188–1194.
13 A. K. Padhi, K. S. Nanjundaswamy and J. B. Goodenough, *ECS Meeting Abstract, No. 58*, Los Angeles, CA., May 5–10, 1996, vol. 96-1.
14 J. B. Goodenough, A. K. Padhi, K. S. Nanjundaswamy and C. Masquelier. *US Pat.*, 5910382, 1999.
15 A. Michel, J. B. Goodenough, A. K. Padhi, K. S. Nanjundaswamy and C. Masquelier. *US Pat.*, 6514640, 2003
16 J.-M. Tarascon and M. Armand, *Nature*, 2001, **414**, 359–367.
17 L. X. Yuan, Z. H. Wang, W. X. Zhang, X. L. Hu, J. T. Chen, Y. H. Huang and J. B. Goodenough, *Energy Environ. Sci.*, 2011, **4**, 269–284.
18 Y. Wang, P. He and H. Zhou, *Energy Environ. Sci.*, 2011, **4**, 805–817.
19 Y. D. Cho, G. T. K. Fey and H. M. Kao, *J. Power Sources*, 2009, **189**, 256–262.
20 S. Okada, S. Sawa, M. Egashira, J. Yamaki, M. Tabuchi, H. Kageyama, T. Konishi and A. Yoshino, *J. Power Sources*, 2001, **97–98**, 430–432.
21 S. Y. Chung, J. T. Bloking and Y. M. Chiang, *Nat. Mater.*, 2002, **1**, 123–126.
22 J. Molenda, A. Stoklosa and T. Bak, *Solid State Ionics*, 1989, **36**, 53–58.
23 Y. Shimakawas, T. Numata and J. Tabuchi, *J. Solid State Chem.*, 1997, **131**, 138–143.
24 B. L. Ellis, K. T. Lee and L. F. Nazar, *Chem. Mater.*, 2010, **22**, 691–714.
25 M. S. Islam, D. J. Driscoll, C. A. J. Fisher and P. R. Slater, *Chem. Mater.*, 2005, **17**, 5085–5092.
26 H. Fang, Z. Pan, L. Li, Y. Yang, G. Yan, G. Li and S. Wei, *Electrochem. Commun.*, 2008, **10**, 1071–1073.
27 J. Xie, N. Imanishi, T. Zhang, A. Hirano, Y. Takeda and O. Yamamoto, *Electrochim. Acta*, 2009, **54**, 4631–4637.
28 C. Wang and J. Hong, *Electrochem. Solid-State Lett.*, 2007, **10**, A65–A69.
29 V. Srinivasan and J. Newman, *Electrochem. Solid-State Lett.*, 2006, **9**, A110–A114.
30 C. Delmas, M. Maccario, L. Croguennec, F. L. Cras and F. Weill, *Nat. Mater.*, 2008, **7**, 665–671.
31 C. Delacourt, P. Poizot, J.-M. Tarason and C. Masquelier, *Nat. Mater.*, 2005, **4**, 254–260.
32 S. Yang, Y. Song, K. Ngala, P. Y. Zavalij and M. S. Whittingham, *J. Power Sources*, 2003, **119**, 239–246.
33 G. Sun, G. Sun, E. Jin, H. B. Gu and Q. Jiang, *J. Appl. Electrochem.*, 2011, **41**, 99–106.
34 K. Saravanan, P. Balaya, M. V. Reddy, B. V. R. Chowdari and J. J. Vittal, *Energy Environ. Sci.*, 2010, **3**, 457–464.
35 R. Malik, D. Burch, M. Bazant and G. Ceder, *Nano Lett.*, 2010, **10**, 4123–4127.
36 A. S. Arico, P. G. Bruce, B. Scrosati, J. M. Tarascon and W. Van Schalkwijc, *Nat. Mater.*, 2005, **4**, 366–377.
37 P. G. Bruce, B. Scrosati and J. M. Tarascon, *Angew. Chem., Int. Ed.*, 2008, **47**, 2930–2946.
38 A. S. Andersson, J. O. Thomas, B. Kalska and L. Haggstrom, *Electrochem. Solid-State Lett.*, 2000, **3**, 66–68.
39 C. Delacourt, PhD thesis, University Picardie—Jules Verne, 2005.
40 N. Meethong, Y. H. Kao, M. Tang, H.-Y. Huang, W. C. Carter and Y.-M. Chiang, *Chem. Mater.*, 2008, **20**, 6189–6198.
41 N. Meethong, H. Y. S. Huang, W. C. Carter and Y.-M. Chiang, *Electrochem. Solid-State Lett.*, 2007, **10**, A134–A138.
42 W. J. Zhang, *J. Power Sources*, 2011, **196**, 2962–2970.
43 W. J. Zhang, *J. Electrochem. Soc.*, 2010, **157**, A1040–A1046.
44 S. F. Yang, P. Y. Zavalij and M. S. Whittingham, *Electrochem. Commun.*, 2001, **3**, 505–508.
45 F. Croce, A. D. Epifanio, J. Hassoun, A. D. T. Olczac and B. Scrosati, *Electrochem. Solid-State Lett.*, 2002, **5**, A47–A50.
46 A. Fedorková, R. Oriňáková, A. Oriňák, H.-D. Wiemhöfer, D. Kaniansky and M. Winter, *J. Solid State Electrochem.*, 2009, **14**, 2173–2178.
47 D. Lepage, C. Michot, G. Liang, M. Gauthier and S. B. Schougaard, *Angew. Chem., Int. Ed.*, 2011, **50**, 6884–6887.
48 Y. H. Huang and J. B. Goodenough, *Chem. Mater.*, 2008, **20**, 7237–7241.
49 www.phostechlithium.com.
50 N. Ravet, J. B. Goodenough, S. Besner, M. Simoneau, P. Hovington and M. Armand, *The Electrochemical Society Meeting*, Honolulu, HI, Oct. 17–22, 1999, vol. 99–2, Abstract 127.
51 N. Ravet, S. Besner, M. Simoneau, A. Vallée, M. Armand and J. F. Magnan, *US Pat.*, 6855273, 2005; 6962666, 2005; and 7344659, 2008.
52 N. Ravet, Y. Chouinard, J. F. Magnan, S. Besner, M. Gauthier and M. Armand, *J. Power Sources*, 2001, **97–98**, 503–507.
53 H. Huang, S. C. Yin and L. F. Nazar, *Electrochem. Solid-State Lett.*, 2001, **4**, A170–A172.
54 N. Ravet, J.-F. Magnan, M. Gauthier and M. Armand, *International Conference on Materials for Advanced Technologies (ICMAT 2001)*, MRS Singapore, July 1–6, 2001.
55 M. Armand, M. Gauthier, J. F. Magnan and N. Ravet, PCT WO 02/27823 and WO 01/27824.
56 M. Gauthier, D. Geoffroy, M. Armand and N. Ravet, *The 20th International Seminar on Primary and Secondary Batteries*, Florida Educational Seminar Inc., Boca Raton, Florida, USA, March 17–20, 2003, www.POWERSOURCES.NET, info@powersources.net or from the authors.
57 C. Zhu, Y. Yu, L. Gu, K. Weichert and J. Maier, *Angew. Chem., Int. Ed.*, 2011, **50**, 6278–9282.
58 K. Saravanan, J. J. Vittal, M. V. Reddy, B. V. R. Chowdari and P. Balaya, *J. Solid State Electrochem.*, 2010, **14**, 1755–1760.
59 D. D. McNeil, L. Devigne, C. Michot, I. Rodigues, G. Liang and M. Gauthier, *J. Electrochem. Soc.*, 2010, **157**, A463–A468.
60 R. Dominko, M. Gaberscek, J. Drofenik, M. Bele, S. Pejovnik and J. Jamnik, *J. Power Sources*, 2003, **119–121**, 770–773.
61 C. Delacourt, P. Poizot, S. Levasseur and C. Masqueliera, *Electrochem. Solid-State Lett.*, 2006, **9**, A352–A355.
62 D.-H. Kim and J. Kim, *Electrochem. Solid-State Lett.*, 2006, **9**, A439–A442.
63 S. Y. Chung, J. T. Bloking and Y. M. Chiang, *Nat. Mater.*, 2002, **1**, 123–128.
64 N. Ravet, A. Abouimrane and M. Armand, *Nat. Mater.*, 2003, **2**, 702.
65 P. Subramanya Herle, B. L. Ellis, N. Coombs and L. F. Nazar, *Nat. Mater.*, 2004, **3**, 147–152.
66 C. A. J. Fisher, V. M. Hart Prieto and M. S. Islam, *Chem. Mater.*, 2008, **20**, 5907–5915.
67 L. Yang, L. Jiao, Y. Miao and H. Yuan, *J. Solid State Electrochem.*, 2009, **13**, 1541–1544.
68 X. Z. Liao, Y. S. He, Z. F. Ma, X. M. Zhang and L. Wang, *J. Power Sources*, 2007, **174**, 720–725.
69 N. Meethong, Y. H. Kao, S. A. Speakman and Y.-M. Chiang, *Adv. Funct. Mater.*, 2009, **19**, 1060–1070.
70 D. Y. Wang, H. Li, S. S. Shi, X. J. Huang and L. Q. Chen, *Electrochim. Acta*, 2005, **50**, 2955–2958.
71 J. Hong, C. S. Wang, X. Chen, S. Upreti and M. S. Whittingham, *Electrochem. Solid-State Lett.*, 2009, **12**, A33–A38.
72 C. Y. Ouyang, D. Y. Wang, S. Q. Shi, Z. X. Wang, H. Li, X. J. Huang and L. Q. Chen, *Chin. Phys. Lett.*, 2006, **23**, 61–65.
73 D. Wang, C. Ouyang, T. Drezen, I. Exnar, A. Kay, N. H. Kwon, P. Gouerec, J. H. Miners, M. Wang and M. Gratzel, *J. Electrochem. Soc.*, 2010, **157**, A225–A229.
74 B. Kang and G. Ceder, *Nature*, 2009, **458**, 190–193.
75 K. Zaghib, J. B. Goodenough, A. Mauger and C. Julien, *J. Power Sources*, 2009, **194**, 1021–1023.
76 G. Ceder and B. Kang, *J. Power Sources*, 2009, **194**, 1024–1028.
77 Y. Jin, C. P. Yang, X. H. Rui, T. Cheng and C. H. Chen, *J. Power Sources*, 2011, **196**, 5623–5630.
78 H.-H. Chang, C.-C. Chang, C.-Y. Su, H.-C. Wu, M.-H. Yang and N.-L. Wu, *J. Power Sources*, 2008, **185**, 466–472.
79 H. Liu, G. X. Wang, D. Wexler, J. Z. Wang and H. K. Liu, *Electrochem. Commun.*, 2008, **10**, 165–169.
80 Z. Chen, Y. Qin, K. Amine and Y.-K. Sun, *J. Mater. Chem.*, 2010, **20**, 7606–7612.

81 X. Meng, D. Geng, J. Liu, R. Li and X. Sun, *Nanotechnology*, 2011, **22**, 165602.
82 X. Meng, Y. Zhong, Y. Sun, M. N. Banis, R. Li and X. Sun, *Carbon*, 2011, **49**, 1133–1144.
83 Y. S. Jung, A. S. Cavanagh, L. A. Riley, S.-H. Kang, A. C. Dillon, M. D. Groner, S. M. George and S.-H. Lee, *Adv. Mater.*, 2010, **22**, 2172–2176.
84 I. D. Scott, Y. S. Jung, A. S. Cavanagh, Y. Yan, A. C. Dillon, S. M. George and S.-H. Lee, *Nano Lett.*, 2011, **11**, 414–418.
85 O. Toprakci, H. A. K. Toprakci, L. Ji and X. Zhang, *KONA Powder and Particle J.*, 2010, **8**, 50–73.
86 H. H. Chang, C. C. Chang, H. C. Wu, Z. Z. Guo, M. H. Yang, Y. P. Chiang, H. S. Sheu and N. L. Wu, *J. Power Sources*, 2006, **158**, 550–556.
87 A. F. Liu, Z. H. Hu, Z. B. Wen, L. Lei and J. An, *Ionics*, 2010, **16**, 311–316.
88 J. K. Kim, G. Cheruvally, J. W. Choi, J. U. Kim, J. H. Ahn, G. B. Cho, K. W. Kim and H. J. Ahn, *J. Power Sources*, 2007, **166**, 211–218.
89 H. F. Xiang, D. W. Zhang, Y. Jin, C. H. Chen, J. S. Wu and H. H. Wang, *J. Mater. Sci.*, 2011, **46**, 4906–4912.
90 H. Yang, X. L. Wu, M. H. Cao and Y. G. Guo, *J. Phys. Chem. C*, 2009, **113**, 3345–3351.
91 N. Recham, L. Dupont, M. Courty, K. Djellab, D. Larcher, M. Armand and J.-M. Tarascon, *Chem. Mater.*, 2009, **21**, 1096–1107.
92 F. Yu, J. J. Zhang, Y. F. Yang and G. Z. Song, *J. Power Sources*, 2010, **195**, 6873–6878.
93 K. S. Park, J. T. Son, H. T. Chung, S. J. Kim, C. H. Lee and H. G. Kim, *Electrochem. Commun.*, 2003, **5**, 839–842.
94 T. N. L. Doan and I. Taniguchi, *J. Power Sources*, 2011, **196**, 1399–1408.
95 A. A. Salah, A. Mauger, K. Zaghib, J. B. Goodenough, N. Ravet, M. Gauthier, F. Gendron and C. M. Julien, *J. Electrochem. Soc.*, 2006, **153**, A1692–A1701.
96 N. Ravet, M. Gauthier, K. Zaghib, J. B. Goodenough, A. Mauger, F. Gendron and C. M. Julien, *Chem. Mater.*, 2007, **19**, 2595–2602.
97 Z. Chen and J. R. Dahn, *J. Electrochem. Soc.*, 2002, **149**, A1184–A1189.
98 Z. R. Chang, H. J. Lv, H. W. Tang, H. J. Li, X. Z. Yuan and H. Wang, *Electrochim. Acta*, 2009, **54**, 4595–4599.
99 Z. Liu, X. Zhang and L. Hong, *J. Appl. Electrochem.*, 2009, **39**, 2433–2438.
100 T. Takeuchi, M. Tabuchi, A. Nakashima, T. Nakamura, Y. Miwa, H. Kageyama and K. Tatsumi, *J. Power Sources*, 2005, **146**, 575–579.
101 M. E. Zhong and Z. T. Zhou, *Mater. Chem. Phys.*, 2010, **119**, 428–431.
102 S. W. Oh, H. J. Bang, S. T. Myung, Y. C. Bae, S. M. Lee and Y. K. Sun, *J. Electrochem. Soc.*, 2008, **155**, A414–A420.
103 S. W. Oh, S. T. Myung, H. J. Bang, C. S. Yoon, K. Amine and Y. K. Sun, *Electrochem. Solid-State Lett.*, 2009, **12**, A181–A185.
104 S. W. Oh, S. T. Myung, S. M. Oh, K. H. Oh, K. Amine, B. Scrosati and Y. K. Sun, *Adv. Mater.*, 2010, **22**, 4842–4845.
105 S. W. Oh, S. T. Myung, S. M. Oh, C. S. Yoon, K. Amine and Y. K. Sun, *Electrochim. Acta*, 2010, **55**, 1193–1199.
106 H. Liu, C. Li, H. P. Zhang, L. J. Fu, Y. P. Wu and H. Q. Wu, *J. Power Sources*, 2006, **159**, 717–720.
107 J. M. Chen, C. H. Hsu, Y. R. Lin, M. H. Hsiaoa and G. T. K. Fey, *J. Power Sources*, 2008, **184**, 498–502.
108 B. Jin, E. M. Jin, K. H. Park and H. B. Gu, *Electrochem. Commun.*, 2008, **10**, 1537–1540.
109 Z. Y. Chen, H. L. Zhu, W. Zhu, J. L. Zhang and Q. F. Li, *Trans. Nonferrous Met. Soc. China*, 2010, **20**, 614–618.
110 D. Zane, M. Carewska, S. Scaccia, F. Cardellini and P. P. Prosin, *Electrochim. Acta*, 2004, **49**, 4259–4271.
111 Y. Wang, Y. Wang, E. Hosono, K. Wang and H. Zhou, *Angew. Chem., Int. Ed.*, 2008, **47**, 7461–7465.
112 X. Yan, G. Yang, J. Liu, Y. Ge, H. Xie, X. Pan and R. Wang, *Electrochim. Acta*, 2009, **54**, 5770–5774.
113 J. Liu, J. Wang, X. Yan, X. Zhang, G. Yang, A. F. Jalbout and R. Wang, *Electrochim. Acta*, 2009, **54**, 5656–5659.
114 X. Zhi, G. Liang, L. Wang, X. Ou, J. Zhang and J. Cui, *J. Power Sources*, 2009, **189**, 779–782.
115 P. P. Prosini, D. Zane and M. Pasquali, *Electrochim. Acta*, 2001, **46**, 3517–3523.
116 Z. Chen and J. R. Dahn, *J. Electrochem. Soc.*, 2002, **149**, A1184–A1189.
117 K. Zaghib, J. Shim, A. Guerfi, P. Charest and K. A. Striebel, *Electrochem. Solid-State Lett.*, 2005, **8**, A207–A210.
118 S. S. Zhang, J. L. Allen, K. Xua and T. R. Jow, *J. Power Sources*, 2005, **147**, 234–240.
119 E. M. Jin, B. Jin, D. K. Jun, K. H. Park, H. B. Gu and K. W. Kim, *J. Power Sources*, 2008, **178**, 801–806.
120 Y. Zhang, H. Feng, X. Wu, L. Wang, A. Zhang, T. Xia, H. Dong and M. Liu, *Electrochim. Acta*, 2009, **54**, 3206–3210.
121 C. Z. Lu, G. Ting-Kuo Fey and H. M. Kao, *J. Power Sources*, 2009, **189**, 155–162.
122 Z. R. Chang, H. J. Lv, H. W. Tang, H. J. Li, X. Z. Yuan and H. Wang, *Electrochim. Acta*, 2009, **54**, 4595–4599.
123 H. Gabrisch, J. D. Wilcox and M. M. Doeff, *Electrochem. Solid-State Lett.*, 2006, **9**, A360–A363.
124 Y. Lin, M. X. Gao, D. Zhu, Y. F. Liu and H. G. Pan, *J. Power Sources*, 2008, **184**, 444–448.
125 R. Dominko, M. Bele, M. Gaberscek, M. Remskar, D. Hanzel, S. Pejovnik and J. Jamnik, *J. Electrochem. Soc.*, 2005, **152**, A607–A610.
126 Y. D. Cho, G. T. K. Fey and H. M. Kao, *J. Power Sources*, 2009, **189**, 256–262.
127 B. Zhao, Y. Jiang, H. Zhang, H. Tao, M. Zhong and Z. Jiao, *J. Power Sources*, 2009, **189**, 462–466.
128 Y. Hu, M. M. Doeff, R. Kostecki and R. Finones, *J. Electrochem. Soc.*, 2004, **151**, A1279–A1285.
129 M. M. Doeff, Y. Hu, F. McLarnon and R. Kostecki, *Electrochem. Solid-State Lett.*, 2003, **6**, A207–A209.
130 J. D. Wilcox, M. M. Doeff, M. Marcinek and R. Kostec, *J. Electrochem. Soc.*, 2007, **154**, A389–A395.
131 M. M. Doeff, J. D. Wilcox, R. Kostecki and G. Lau, *J. Power Sources*, 2006, **163**, 180–184.
132 H. C. Shin, W. I. I. CHo and H. Jang, *Electrochim. Acta*, 2006, **52**, 1472–1476.
133 J. K. Kim, J. W. Choi, G. S. Chauhan, J. H. Ahn, G. C. Hwang, J. B. Choi and H. J. Ahn, *Electrochim. Acta*, 2008, **53**, 8258–8264.
134 T. Nakamura, Y. Miwa, M. Tabuchi and Y. Yamada, *J. Electrochem. Soc.*, 2006, **153**, A1108–A1114.
135 C. W. Ong, Y. K. Lin and J. S. Chen, *J. Electrochem. Soc.*, 2007, **154**, A527–A533.
136 Y. H. Nien, J. R. Carey and J. S. Chen, *J. Power Sources*, 2009, **193**, 822–827.
137 J. Chen, J. Z. Wang, A. I. Minett, Y. Liu, C. Lynam, H. Liu and G. G. Wallace, *Energy Environ. Sci.*, 2009, **2**, 393–396.
138 H. Zhang, G. Cao and Y. Yang, *Energy Environ. Sci.*, 2009, **2**, 932–943.
139 Y. Liu, X. Li, H. Guo, Z. Wang, W. Peng, Y. Yang and R. Liang, *J. Power Sources*, 2008, **184**, 522–526.
140 L. Wang, Y. Huang, R. Jiang and D. Jia, *J. Electrochem. Soc.*, 2007, **154**, A1015–A1019.
141 J. J. Chen and M. S. Whittingham, *Electrochem. Commun.*, 2006, **8**, 855–858.
142 Y. Zhou, J. Wang, Y. Hu, R. O'Hayre and Z. Shao, *Chem. Commun.*, 2010, **46**, 7151–7153.
143 X. L. Li, F. Y. Kang, X. D. Bai and W. C. Shen, *Electrochem. Commun.*, 2007, **9**, 663–666.
144 M. S. Bhuvaneswari, N. N. Bramnik, D. Ensling, H. Ehrenberg and W. Jaegermann, *J. Power Sources*, 2008, **180**, 553–560.
145 F. Y. Su, C. You, Y. B. He, W. Lv, W. Cui, F. Jin, B. Li, Q. H. Yang and F. Kang, *J. Mater. Chem.*, 2010, **20**, 9644–9650.
146 Y. Ding, Y. Jiang, F. Xu, J. Yin, H. Ren, Q. Zhuo, Z. Long and P. Zhang, *Electrochem. Commun.*, 2010, **12**, 10–13.
147 X. Zhou, F. Wang, Y. Zhu and Z. Liu, *J. Mater. Chem.*, 2011, **21**, 3353–3358.
148 L. Wang, H. Wang, Z. Liu, C. Xiao, S. Dong, P. Han, Z. Zhang, X. Zhang, C. Bi and G. Cui, *Solid State Ionics*, 2010, **181**, 1685–1689.
149 J. K. Kim, G. Cheruvally, J. H. Ahn and H. J. Ahn, *J. Phys. Chem. Solids*, 2008, **29**, 1257–1260.
150 Y. Liu, C. Cao and J. Li, *Electrochim. Acta*, 2010, **55**, 3921–3926.
151 T. Muraliganth, A. V. Murugan and A. Manthiram, *J. Mater. Chem.*, 2008, **18**, 5661–5668.

152 X. L. Wu, L. Y. Jiang, F. F. Cao, Y. G. Guo and L. J. Wan, *Adv. Mater.*, 2009, **21**, 2710–2714.
153 C. R. Sides, F. Croce, V. Y. Young, C. R. Martin and B. Scrosati, *Electrochem. Solid-State Lett.*, 2005, **8**, A484–A487.
154 C. M. Doherty, R. A. Caruso, B. M. Smarsly, P. Adelhelm and C. J. Drummond, *Chem. Mater.*, 2009, **21**, 5300–5306.
155 M. R. Yang, W. H. Ke and S. H. Wu, *J. Power Sources*, 2005, **146**, 539–543.
156 L. N. Wang, X. C. Zhan, Z. G. Zhang and K. L. Zhang, *J. Alloys Compd.*, 2008, **456**, 461–465.
157 W. Zhou, W. He, Z. Li, H. Zhao and S. Yan, *J. Solid State Electrochem.*, 2009, **13**, 1819–1823.
158 M. Gaberscek, R. Dominko, M. Bele, M. Remskar, D. Hanzel and J. Jamnik, *Solid State Ionics*, 2005, **176**, 1801–1805.
159 F. Yu, J. Zhang, Y. Yang and G. Song, *J. Power Sources*, 2009, **189**, 794–797.
160 K. Wang, R. Cai, T. Yuan, X. Yu, R. Ran and Z. Shao, *Electrochim. Acta*, 2009, **54**, 2861–2868.
161 Z. Chen, H. Zhu, S. Ji, R. Fakir and V. Linkov, *Solid State Ionics*, 2008, **179**, 1810–1815.
162 C. Lai, Q. Xu, H. Ge, G. Zhou and J. Xie, *Solid State Ionics*, 2008, **179**, 1736–1739.
163 X. Yan, G. Yang, J. Liu, Y. Ge, H. Xie, X. Pan and R. Wang, *Electrochim. Acta*, 2009, **54**, 5770–5774.
164 D. Zhang, X. Yu, Y. Wang, R. Cai, Z. Shao, X. Z. Liao and Z. F. Ma, *J. Electrochem. Soc.*, 2009, **156**, A802–A808.
165 G. Ting-Kuo Fey, T. L. Lu, F. Y. Wu and W. H. Li, *J. Solid State Electrochem.*, 2008, **12**, 825–833.
166 G. Ting-Kuo Fey and T. L. Lu, *J. Power Sources*, 2008, **178**, 807–814.
167 C. W. Ong, Y. K. Lin and J. S. Chen, *J. Electrochem. Soc.*, 2007, **154**, A527–A533.
168 Y. H. Nien, J. R. Carey and J. S. Chen, *J. Power Sources*, 2009, **193**, 822–827.
169 P. Subramanya-Herle, B. Ellis, N. Coombs and L. F. Nazar, *Nat. Mater.*, 2004, **3**, 147–152.
170 Y. H. Rho, L. F. Nazar, L. Perry and D. Ryan, *J. Electrochem. Soc.*, 2007, **154**, A283–A289.
171 G. Lewis and C. E. Myers, *J. Phys. Chem.*, 1963, **67**, 1289–1292.
172 Y. Xu, Y. Lu, L. Yan, Z. Yang and R. Yang, *J. Power Sources*, 2006, **160**, 570–576.
173 Y. Lin, M. X. Gao, D. Zhu, Y. F. Liu and H. G. Pan, *J. Power Sources*, 2008, **184**, 444–448.
174 M. Gauthier, C. Michot, N. Ravet, J. Dufour, G. Liang, J. Wontcheu, L. Gauthier and D. D. McNeil, *J. Electrochem. Soc.*, 2010, **157**, A453–A462.
175 J. F. Ni, H. H. Zhou, J. T. Chen and X. X. Zhang, *Mater. Lett.*, 2007, **61**, 1260–1264.
176 S. S. Zhang, J. L. Allen, K. Xu and T. R. Jow, *J. Power Sources*, 2005, **147**, 234–240.
177 G. T. K. Fey, T. L. Lu, F. Y. Wu and W. H. Li, *J. Solid State Electrochem.*, 2008, **12**, 825–833.
178 H. Liu, C. Li, H. P. Zhang, L. J. Fu, Y. P. Wu and H. Q. Wu, *J. Power Sources*, 2006, **159**, 717–720.
179 Y. Z. Dong, Y. M. Zhao, Y. H. Chen, Z. F. He and Q. Kuang, *Mater. Chem. Phys.*, 2009, **115**, 245–250.
180 J. Barker, M. Y. Saidi and J. L. Swoyer, *Electrochem. Solid-State Lett.*, 2003, **6**, A53–A55.
181 H. P. Liu, Z. X. Wang, X. H. Li, H. J. Guo, W. J. Peng, Y. H. Zhang and Q. Y. Hu, *J. Power Sources*, 2008, **184**, 469–472.
182 L. Wang, G. C. Liang, X. Q. Ou, X. K. Zhi, J. P. Zhang and J. Y. Cui, *J. Power Sources*, 2009, **189**, 423–428.
183 X. Zhi, G. Liang, L. Wang, X. Ou, J. Zhang and J. Cui, *J. Power Sources*, 2009, **189**, 779–782.
184 X. F. Guo, H. Zhan and Y. H. Zhou, *Solid State Ionics*, 2009, **180**, 386–391.
185 S. Beninati, L. Damen and M. Mastragostino, *J. Power Sources*, 2009, **194**, 1094–1098.
186 K. F. Hsu, S. Y. Tsay and B. J. Hwang, *J. Mater. Chem.*, 2004, **14**, 2690–2695.
187 J. K. Kim, J. W. Choi, G. S. Chauhan, J. H. Ahn, G. C. Hwang, J. B. Choi and H. J. Ahn, *Electrochim. Acta*, 2008, **53**, 8258–8264.
188 D. Choi and P. N. Kumta, *J. Power Sources*, 2007, **163**, 1064–1069.
189 Y. Lin, M. X. Gao, D. Zhu, Y. F. Liu and H. G. Pan, *J. Power Sources*, 2008, **184**, 444–448.
190 N. J. Yun, H. W. Ha, K. H. Jeong, H. Y. Park and K. Kim, *J. Power Sources*, 2006, **160**, 1361–1368.
191 J. S. Yang and J. J. Xu, *Electrochem. Solid-State Lett.*, 2004, **7**, A515–A518.
192 K. F. Hsu, S. Y. Tsay and B. J. Hwang, *J. Mater. Chem.*, 2004, **14**, 2690–2695.
193 A. Vadivel Murugan, T. Muraliganth and A. Manthiram, *J. Electrochem. Soc.*, 2009, **156**, A79–A83.
194 A. Vadivel Murugan, T. Muraliganth and A. Manthiram, *J. Phys. Chem. C*, 2008, **112**, 14665–14671.
195 Y. Li, C. Wan, Y. Wu, C. Jiang and Y. Zhu, *J. Power Sources*, 2000, **85**, 294–298.
196 K. Matsuda and I. Taniguchi, *J. Power Sources*, 2004, **132**, 156–160.
197 S. H. Park, S. W. Oh and Y. K. Sun, *J. Power Sources*, 2005, **146**, 622–625.
198 S. H. Park, S. W. Oh, S. T. Myung, Y. C. Kang and Y. K. Sun, *Solid State Ionics*, 2005, **176**, 481–486.
199 S. H. Ju and Y. C. Kang, *Mater. Chem. Phys.*, 2008, **107**, 328–333.
200 S. L. Bewlay, K. Konstantinov, G. X. Wang, S. X. Dou and H. K. Liu, *Mater. Lett.*, 2004, **58**, 1788–1791.
201 K. Konstantinov, S. L. Bewlay, G. X. Wang, M. Lindsay, J. Z. Wang, H. K. Liu, S. X. Dou and J. H. Ahn, *Electrochim. Acta*, 2004, **50**, 421–426.
202 M. Konarova and I. Taniguchi, *Powder Technol.*, 2009, **191**, 111–116.
203 M. Konarova and I. Taniguchi, *J. Power Sources*, 2009, **194**, 1029–1035.
204 M. R. Yang, T. H. Teng and S. H. Wu, *J. Power Sources*, 2006, **159**, 307–311.
205 K. Tang, J. Sun, X. Yu, H. Li and X. Huang, *Electrochim. Acta*, 2009, **54**, 6565–6569.
206 C. Yada, Y. Iriyama, S. K. Jeong, T. Abe, M. Inaba and Z. Ogumi, *J. Power Sources*, 2005, **146**, 559–564.
207 S. W. Song, R. P. Reade, R. Kostecki and K. Striebel, *J. Electrochem. Soc.*, 2006, **153**, A12–A16.
208 F. Sauvage, E. Baudrin, L. Gengembre and J. M. Tarascon, *Solid State Ionics*, 2005, **176**, 1869–1876.
209 K. F. Chiu, *J. Electrochem. Soc.*, 2007, **154**, A129–A133.
210 J. Hong, C. S. Wang, N. J. Dudney and M. J. Lance, *J. Electrochem. Soc.*, 2007, **154**, A805–A809.
211 J. Ma and Q. Z. Qin, *J. Power Sources*, 2005, **148**, 66–71.
212 Z. G. Lu, M. F. Lo and C. Y. Chung, *J. Phys. Chem. C*, 2008, **112**, 7069–7078.
213 J. Xie, N. Imanishi, T. Zhang, A. Hirano, Y. Takeda and O. Yamamoto, *Electrochim. Acta*, 2009, **54**, 4631–4637.
214 H. Liu, C. Li, H. P. Zhang, L. J. Fu, Y. P. Wu and H. Q. Wu, *J. Power Sources*, 2006, **159**, 717–720.
215 X. J. Zhu, L. B. Cheng, C. G. Wang, Z. P. Guo, P. Zhang, G. D. Du and H. K. Liu, *J. Phys. Chem. C*, 2009, **113**, 14518–14522.
216 M. Balasubramanian, X. Sun, X. Q. Yang and J. McBreen, *J. Power Sources*, 2001, **92**, 1–8.
217 W. S. Yoon, K. Y. Chung, J. Mcbreen, K. Zaghib and X. Q. Yang, *Electrochem. Solid-State Lett.*, 2006, **9**, A415–A417.
218 H. C. Shin, K. W. Nam, W. Y. Chang, B. W. Cho, W. S. Yoon, X. Q. Yang and K. Y. Chung, *Electrochim. Acta*, 2011, **56**, 1182–1189.
219 D. Jugovic and D. Uskokovic, *J. Power Sources*, 2009, **190**, 538–544.
220 H. C. Kang, D. K. Jun, B. Jin, E. M. Jin, K. H. Park, H. B. Gu and K. W. Kim, *J. Power Sources*, 2008, **179**, 340–346.
221 X. Qin, X. H. Wang, H. M. Xiang, J. Xie, J. J. Li and Y. C. Zhou, *J. Phys. Chem. C*, 2010, **114**, 16806–16812.
222 G. Yang, H. M. Ji, H. D. Liu, K. F. Huo, J. J. Fu and P. K. Chu, *J. Nanosci. Nanotechnol.*, 2010, **10**, 980–986.
223 H. Nakano, K. Dokko, S. Koizumi, H. Tannai and K. Kanamura, *J. Electrochem. Soc.*, 2008, **155**, A909–A914.